



Review

A Comprehensive Assessment of Right Ventricular Function in Chronic Thromboembolic Pulmonary Hypertension

Stella Marchetta ¹, Tom Verbelen ² , Guido Claessen ³, Rozenn Quarck ⁴ , Marion Delcroix ^{4,5} and Laurent Godinas ^{4,5,*}

¹ Department of Cardiology, CHC Mont-Légia, 4000 Liège, Belgium

² Department of Cardiac Surgery, University Hospitals Leuven, 3000 Leuven, Belgium

³ Department of Cardiology, University Hospitals Leuven, 3000 Leuven, Belgium

⁴ Laboratory of Respiratory Diseases and Thoracic Surgery (BREATHE), Department of Chronic Diseases and Metabolism (CHROMETA), KU Leuven, 3000 Leuven, Belgium

⁵ Department of Pneumology, University Hospitals Leuven, 3000 Leuven, Belgium

* Correspondence: laurent.godinas@uzleuven.be

Abstract: While chronic thromboembolic pulmonary hypertension (CTEPH) results from macroscopic and microscopic obstruction of the pulmonary vascular bed, the function of the right ventricle (RV) and increased RV afterload are the main determinants of its symptoms and prognosis. In this review, we assess RV function in patients diagnosed with CTEPH with a focus on the contributions of RV afterload and dysfunction to the pathogenesis of this disease. We will also discuss changes in RV function and geometry in response to treatment, including medical therapy, pulmonary endarterectomy, and balloon pulmonary angioplasty.

Keywords: chronic thromboembolic pulmonary hypertension; right ventricle; echocardiography; cardiac magnetic resonance imaging



Citation: Marchetta, S.; Verbelen, T.; Claessen, G.; Quarck, R.; Delcroix, M.; Godinas, L. A Comprehensive Assessment of Right Ventricular Function in Chronic Thromboembolic Pulmonary Hypertension. *J. Clin. Med.* **2023**, *12*, 47. <https://doi.org/10.3390/jcm12010047>

Academic Editor: Andrea Dell'Amore

Received: 8 November 2022

Revised: 13 December 2022

Accepted: 14 December 2022

Published: 21 December 2022



Copyright: © 2022 by the authors. Licensee MDPI, Basel, Switzerland. This article is an open access article distributed under the terms and conditions of the Creative Commons Attribution (CC BY) license (<https://creativecommons.org/licenses/by/4.0/>).

1. Introduction

Chronic thromboembolic pulmonary hypertension (CTEPH) is diagnosed in patients presenting with precapillary pulmonary hypertension (PH) with an increased mean pulmonary artery pressure (mPAP) > 20 mmHg at rest, a pulmonary artery wedge pressure (PAWP) ≤ 15 mmHg, and a pulmonary vascular resistance (PVR) > 2 WU [1], together with symptoms and persistence of segmental perfusion defects after three months of effective anticoagulation [2]. Patients with relevant symptoms and segmental perfusion defects in the absence of the aforementioned hemodynamic criteria are diagnosed with chronic thromboembolic pulmonary disease (CTEPD) [2]. CTEPH is classified as PH group 4 in the European Society of Cardiology (ESC)/European Respiratory Society (ERS) guidelines (i.e., PH secondary to pulmonary artery obstruction) [1]. While the incidence of CTEPH varies widely, it is typically diagnosed in 2–3% of patients who have recovered from an acute pulmonary embolism (APE) [3,4].

The persistence of fibro-thrombotic material in the pulmonary vascular bed results in increased PVR and right ventricle (RV) afterload [5]. As the disease progresses, the mPAP increases to maintain blood flow. While the RV initially adapts to the increased afterload, it will eventually become dysfunctional, leading to RV failure [6]. In addition to proximal occlusion of the vascular bed, patients diagnosed with CTEPH frequently develop microvasculopathy [7] due to ongoing shear stress, endothelial dysfunction, and growth of systemic-to-pulmonary anastomoses [5]. Microvasculopathy contributes to the progressive increases in PVR and RV afterload [8].

Current regimens are used to treat CTEPH by targeting the occlusions at various levels [2]. For example, patients with a proximal disease may respond effectively to pulmonary endarterectomy (PEA) which targets and removes occlusions in the main

pulmonary arteries (PAs) [9]. By contrast, patients presenting with more distal lesions may benefit from balloon pulmonary angioplasty (BPA) [10]. Microvasculopathy may be targeted with medical therapy, notably with riociguat, which stimulates soluble guanylate cyclase (sGC) [11].

In this manuscript, we will review the pathophysiology of RV dysfunction in CTEPH, with a particular emphasis on points of clinical relevance and the impact of specific medical and surgical treatments.

2. Pathophysiology of RV Dysfunction in CTEPH

2.1. Pulmonary Vascular Obstruction and Determinants of RV Afterload

The pathophysiological mechanisms underlying CTEPH are complex and include both macroscopic and microscopic changes to the pulmonary vascular bed together with pathophysiological RV responses to the resulting increased afterload (Figure 1). The persistence of fibro-thrombotic material in the lung vasculature increases the PVR and, thus, RV afterload. As the disease progresses, the RV adapts and the mPAP progressively increases to maintain blood flow across the obstructed pulmonary circulation. However, the ability of the RV to adapt will eventually be exceeded. Without effective treatment, the RV will initiate a series of maladaptive responses that will eventually result in right-sided heart failure and death [12]. Of note, the degree of RV afterload that develops is not solely dependent on PVR but also on pulsatile phenomena associated with pulmonary vascular compliance (PVC) and PA impedance (Z) [13] in conjunction with wave reflection and inertance of blood.

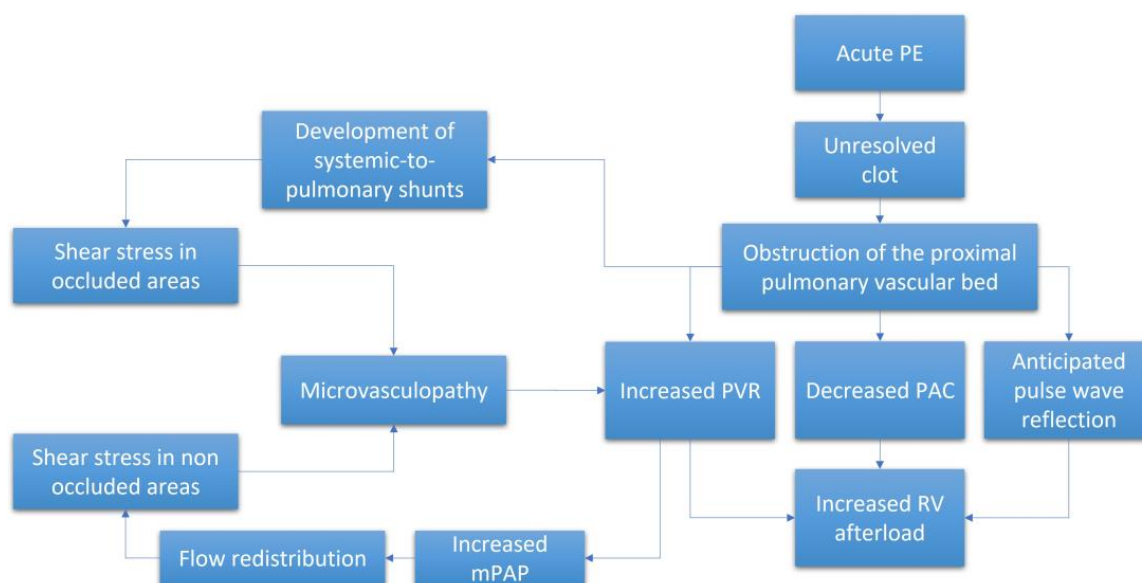


Figure 1. Schematic representation of the pathophysiological process leading to the increased RV afterload. APE = acute pulmonary embolism. mPAP = mean pulmonary artery pressure. PAC = pulmonary artery compliance. PVR = pulmonary vascular resistance. RV = right ventricle.

Some researchers have suggested that differences in these hemodynamic responses might be used to differentiate between CTEPH, characterized by a proximal macroscopic obstruction and pulmonary arterial hypertension (PAH), in which obstruction is limited to the distal pulmonary vessels with a diameter of less than 1 mm. This point remains controversial. Results from previous studies revealed that an early pulse wave reflection in CTEPH was the result of increased stiffness of the proximal PA [14]. This anticipated wave reflection, which normally reaches the pulmonary valve during diastole, crosses the forward pulse wave at systole; this results in an overall increase in pulse pressure due to the summation of both backward and forward waves. The overall impact of this summation would be decreased blood flow and a net increase in RV workload [14–17]. However, these

results were not entirely confirmed by results from another study, in which a high-fidelity transducer catheter was used to generate pressure measurements in both CTEPH and PAH patients with the same levels of mPAP [18]. While different abnormal pressure-wave reflections were detected when comparing both groups of patients, with results indicating increases in anticipated wave reflection specifically in CTEPH patients, these differences were not sufficient to discriminate between these two diseases. Similarly, results from large animal model studies revealed that pulse pressures and the pulsatile component of RV hydraulic load increased in response to proximal obstruction accompanied by decreases in PVC [19]. However, this model focuses on acute obstruction and thus does not take into account the structural alterations encountered in response to distended proximal circulation that typically results in PH associated with distal obstruction.

Other researchers suggested that patients with CTEPH might exhibit higher PA pulse pressures compared to those diagnosed with PAH and thus potentially associated with reduced PVC [14]. However, these results were not confirmed in other studies in which PA pulse pressures and PVC were reported to be similar in these two conditions [13,18]. These conflicting results might be due to the extent of microvasculopathy in these diseases; distal (as opposed to proximal) remodeling may elicit a more profoundly impaired vascular response to the flow pulsatility [20]. Finally, the relationship between PVR and PVC (the time constant, RC) undergoes little to no variation in patients diagnosed with precapillary PH [21].

2.2. Role of Microvasculopathy

Microvasculopathy has been detected in both the occluded and non-occluded lung areas in patients with CTEPH [22]. Various mechanisms have been proposed to explain this phenomenon. Among the possible etiologies, the remodeling of small vessels in non-occluded regions may be the result of increased pressure secondary to the occlusion which will result in more blood flow toward non-occluded lung segments; this will ultimately aggravate the ventilation and perfusion mismatch and trigger shear stress [23,24]. Moreover, the exposure of small vessels to high pressure and the release of vasoactive mediators can lead to endothelial dysfunction and microvasculopathy [8]. Impaired angiogenesis and inflammation have also been involved [25]. Recent studies have highlighted the contributions of systemic-to-pulmonary vascular anastomoses in the induction of microvasculopathy within occluded segments of the lungs [7]. Collectively, these processes contribute to the progressive increases in PVR and RV afterload. The microvascular component may also explain why some CTEPH patients do not respond to surgical treatment (PEA or BPA) and why others can be managed effectively with medical therapy [26]. The information provided in Figure 1 summarizes the pathophysiology underlying the observed increase in RV afterload in patients diagnosed with CTEPH.

2.3. RV Adaptation

The RV adapts to progressive increases in afterload via different mechanisms in order to maintain a sufficient cardiac output (CO) at rest and during exercise [27,28]. The adaptive phase is marked by RV remodeling, primarily hypertrophy. This response is consistent with LaPlace's Law; as applied in this case, RV wall thickness must increase to decrease the wall tension triggered by the RV overload. While undergoing concentric hypertrophy, RV function remains preserved, as well as its capacity to adapt during exercise [29]. Likewise, the stroke volume (SV) is maintained due to the increased contractility conferred by adaptive remodeling. At this point, the right ventricular pulmonary arterial coupling (RV-PAC, assessed as the ratio between end-systolic elastance and arterial elastance, or E_{es}/E_a) remains constant and adequate to support critical functions [30]. At the cellular level, increased thickness of the RV wall requires both protein synthesis and an increase in cell size secondary to the addition of sarcomeres [31]. At the onset of the disease, these changes are beneficial; RV remodeling and functional adaptability are major determinants of exercise capacity and survival in patients with CTEPH.

2.4. RV Failure and the Maladaptive Phenotype

When the mechanisms leading to adaptation are ultimately exhausted and the RV has no further capacity to adapt, the RV enters into a phase of maladaptive remodeling with volumetric adaptation [32]. This phase is marked by eccentric hypertrophy, RV chamber enlargement, and ultimately dyssynchrony with the left ventricle (LV) [30]. In this phase, the SV is maintained mainly through the Frank–Starling mechanism. The alteration of RV geometry leads to annular dilatation; this will ultimately result in functional tricuspid regurgitation (TR), which will decrease the RVSV and increase the RV preload. Moreover, given the extent of ventricular interdependence within the pericardial space, marked RV dilatation will alter LV geometry due to a leftward shift of the interventricular septum [33]. This displacement will impair LV diastolic function and exacerbate the decrease in CO. The dyssynchrony that develops between the two ventricles will extend the duration of the RV contraction beyond the closure of the pulmonary valves; this will result in additional increased RV wall stress as well as RV work and mechanical inefficiency [34]. This response will also contribute to the leftward shift of the septum, reduced filling space for the LV, and further decreases in the SV [33]. PH may also result in RV diastolic dysfunction due to cardiomyocyte hypertrophy and myocardial fibrosis, which will result in a progressive increase in RV wall stiffness, RV filling pressures, elevated right atrial pulmonary (RAP) pressures, and venous congestion [35,36]. The RV-PAC progressively evolves toward an inadequate relationship characterized by progressive uncoupling [30]. Furthermore, the decrease in systemic blood flow results in deteriorating coronary perfusion despite the increased oxygen demand that develops in response to RV hypertrophy and increased RV work [37]. Increases in RV wall tension and decreases in RV capillary perfusion will both aggravate ischemia. Progressive cardiac dysfunction ensues, with reductions in RV contractility, local ischemia, and myocardial fibrosis that eventually culminate in RV failure [38]. Collectively, this mechanism and relationships explain why RV function is the main leading prognostic indicator in patients with CTEPH. Figure 2 summarizes the evolution of the RV function in CTEPH.

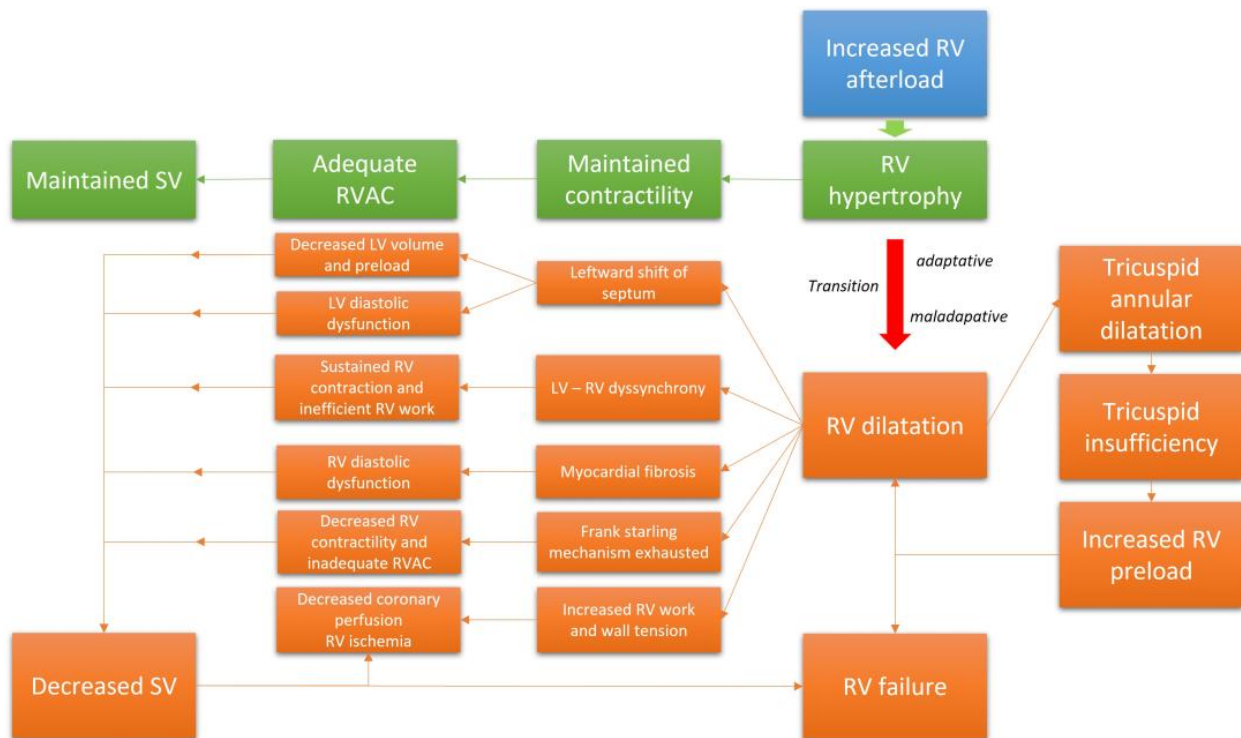


Figure 2. The transition from an adaptive RV phenotype to a maladaptive phenotype.

Exercise results in a dramatic increase in RV work because of the need to increase CO to meet the oxygen requirements of active muscles [39]. Therefore, physical activity will create even greater stress and lead to maladaptive RV changes in addition to those already required to maintain adequate SV and CO at rest [40]. This explains why symptoms are mainly encountered during physical activity in the early phase of the disease.

The cellular and tissue responses and mechanisms underlying the transition from compensated RV remodeling to RV failure are complex and not fully understood [41]. Activation of fetal gene expression and angiogenesis mediated by the hypoxia-inducible factor (HIF), and the vascular endothelial growth factor (VEGF) axis, have both been implicated in RV remodeling [42–44]; inflammatory and immune-mediated mechanisms have also been described [45,46]. Alterations in myocardial metabolism and activation of the neurohumoral system also contribute to the pathophysiology of the RV maladaptive phenotype [47,48]. Among these changes is a metabolic switch from fatty acid oxidation to anaerobic glycolysis, which is a less efficient mechanism used to provide the ATP required for cardiomyocyte contractions. Similarly, myocardial ischemia coupled with inflammation may lead to collagen deposition and local RV fibrosis [36,49,50]. It is critical to recognize that a hypertrophied RV myocardium has an increased need for oxygen provided by the additional blood supply. However, results from human studies and animal models revealed RV hypertrophy resulted in decreased capillary blood flow [51–53] which exacerbated the myocardial ischemia. Collectively, these cellular and molecular abnormalities may trigger mechanisms that lead to fibrosis. In animal models, fibrosis observed in response to maladaptive hypertrophy results from the upregulation of profibrotic growth factors, notably those associated with the TGF- β signaling pathway [54,55]. RV fibrosis has also been detected in cardiac magnetic resonance imaging (cMRI) and histology studies performed in patients with PH [55,56].

While the RV may evolve from an adaptive to a maladaptive phenotype, this change may not be irreversible. A severely dysfunctional RV may improve dramatically in response to significant afterload reduction. This is the underlying rationale for the treatment of CTEPH with PEA, BPA, and potentially lung transplantation. However, it is not clear whether RV function will be fully restored after these treatments, nor do we fully understand what mechanisms might be precluding a complete RV functional repair.

2.5. Clinical Relevance of RV Dysfunction in CTEPH

RV dysfunction is an important factor contributing to the symptoms and decreased exercise capacity in patients diagnosed with PH. However, the symptoms due to RV dysfunction that emerge in patients who develop CTEPH after an acute pulmonary embolism (APE) are highly variable and follow a non-linear trajectory. A wide range of PVR and RV dysfunction may be encountered in patients with the same level of pulmonary vascular obstruction and hemodynamic disturbance. Thus, the nature and relevance of the patient symptoms may change greatly, from nearly asymptomatic CTEPD to the most severe and decompensated presentations of CTEPH. This high variation in hemodynamic presentation precludes direct clinical comparison between patients with CTEPH and those with PAH, as the latter present most frequently with high pulmonary pressures and high levels of PVR.

Several studies have assessed and correlated RV function with symptoms in patients with CTEPH. Among these, persistently increased RV afterload after PEA has been linked to symptoms, including correlations between symptoms and mPAP/CO ratio during exercise [57] and between symptoms and persistence of altered PVC [58]. Abnormal mPAP/CO and RV responses during exercise have also been reported in symptomatic cases of CTEPD [59]. In another study that correlated oxygen consumption (VO_2) with invasive hemodynamic measurements taken during exercise, the cardiac index (CI) was identified as an independent predictor of impaired VO_2 and abnormal functional capacity [60]. Similarly, results of a recent study of RV dysfunction based on four echocardiographic RV parameters revealed an association between these outcomes with symptoms and exercise capacity [61]. Taken together, these studies suggest a fundamental role of RV dysfunction as the source

of clinical symptoms. In addition to RV dysfunction, the dead-space effect and impaired oxygen extraction in the periphery may provide important contributions to the symptoms of CTEPH [62,63].

RV dysfunction triggered by increased afterload is also the major determinant of prognosis in CTEPH. Results from a large multicenter prospective study of 679 patients revealed that the prognosis of CTEPH patients was positively and independently associated with the New York Heart Association (NYHA) functional class, surgery (i.e., removal of endoluminal obstruction), and RV afterload [64]. In patients who did not undergo surgery, RAP pressure, reflecting the degree of RV failure, was an independent factor associated with disease prognosis [64]. Likewise, results from a series of large retrospective studies revealed that high PVR (both pre-operative and early in the post-operative phase), which is mainly driven by low CO, was associated with poor surgical outcomes, risk of residual PH, and reduced survival [65–68]. Similarly, results from prospective studies that included 880 CTEPH patients treated with PEA revealed that a low CI and high RAP pressures measured three to six months after PEA were both negative prognosis factors [67]. Other studies reported that CI during exercise and the slope of the mPAP/CO curve were independent predictors of survival in both PAH and CTEPH [60]. Additionally, the pulmonary artery pulsatility index (PAPi), which is the ratio between the pulse pressure and the RAP, has been proposed as a critical parameter linking PVC and RV function. Interestingly, PAPi was inversely correlated with hemodynamic stability; a low PAPi was identified as a negative prognostic factor in patients diagnosed with CTEPH [69]. Collectively, these studies support our current understanding of RV function as a main prognostic marker in CTEPH.

3. Evaluation of RV Structure and Function in CTEPH

3.1. Right Heart Catheterization (RHC)

RHC remains the “gold standard” for the diagnosis of PH. This method results in accurate measurements of critical pressures, including those measured in the PA (mPAP) and the RA (RAP). Moreover, RHC provides critical information on cardiac function via the direct measurement of CO with either the thermodilution or Fick methods [70]. Assessments of PAP and CO facilitate the calculation of derived measures, including PVR, CI, SV, and PVC. Invasive measurements of the PA flow and RV volumes provide a complex evaluation of pulmonary circulation, including Z and RVAC values, respectively [71,72].

3.2. Echocardiography

Echocardiography remains an important tool that can be used to screen patients for CTEPH after APE in cases with persistent symptoms [73]. The systolic pulmonary arterial pressure (sPAP) is commonly estimated from the rate of tricuspid regurgitation (TR) [74]. TR at a velocity > 2.8 m/s corresponds to an sPAP of ~36 mmHg and suggests the possibility of PH [1].

Echocardiography is also in wide use as a means to assess RV function [61]. Signs of adaptive RV function to increased pressure overload can be detected as a thickening of the free wall of the right ventricle (>5 mm), indicating RV hypertrophy [75]. At later stages, maladaptive RV function is revealed by dilatation of the RV (RV diameter > 42 mm at the base and >35 mm at the mid-level) together with a flattening of the interventricular septum during systole (and/or in diastole in more severe cases) [76]. Other parameters suggesting PH that can be evaluated by echocardiography include PA acceleration time (PAAT), which can be diagnosed by an RV outflow Doppler acceleration time (<105 ms), followed eventually by the presence of a mid-systolic notch, the latter reflecting an anticipated pulse wave reflection [77]. Signs of severe RV dysfunction include dilatation of the RA (>18 cm²) and the inferior vena cava (>21 mm) with decreased inspiratory collapse and hepatic venous reflux [1]. Pericardial effusion may also be detected and is considered to be a sign of very severe disease. RV function can also be assessed based on the tricuspid annular plane systolic excursion (TAPSE, normal value [NV] > 17 mm), tissue

Doppler-derived tricuspid lateral annular systolic velocity (RV-S', NV > 10 cm/s), right ventricular fractional area change (RV-FAC, NV > 35%), and RV myocardial performance index (RV-MPI, NV > 0.4) [75]. Speckle-tracking echocardiography (STE) used to evaluate global longitudinal strain (GLS) of the RV-free wall (RVFW) can provide a highly-sensitive assessment of RV function and local wall contractility [78].

Echocardiography may also be used for a follow-up of CTEPH patients. Results of a recent study revealed the comparatively high sensitivity (68%) and specificity (67%) of transthoracic echocardiography (TTE) for determining the intermediate or high probability of PH and detecting residual PH after PEA [79].

3.3. Cardiac Magnetic Resonance Imaging (cMRI)

Cardiac MRI (cMRI) is a useful alternative to echocardiography for the identification and monitoring of patients with PH and to assess RV function [80]. This method provides accurate information regarding RV mass as well as its function and kinetics. In addition to the anatomical information, cMRI also provides a non-invasive assessment of blood flow, including SV, CO, and PA distensibility. However, this method is somewhat less accurate when used to estimate PAP and PVR. Interestingly, structural abnormalities, including RV fibrosis, can be demonstrated and quantified by late enhancement techniques.

4. Impact of Pulmonary Thromboendarterectomy on RV Function

4.1. RV Structural and Functional Improvement after PEA

PEA is the recommended treatment for patients with CTEPH that is amenable to surgical treatment [1,2]. PEA can be performed to remove an obstruction from the proximal pulmonary vasculature and thus relieve outflow stress on the RV [9,68]. A successful PEA will improve prognosis, symptoms, functional capacity, hemodynamics, and RV function [64,81,82]. Structural and functional RA improvements have been reported early in the history of PEA [83,84], and reverse remodeling is frequently encountered. Comprehensive studies designed to decipher the evolution of RV after PEA have been published [85]. RV volumes, as assessed by echocardiography or cMRI, decrease during the first weeks after the surgery. Invasive hemodynamic measurements also improve with increases in CO and CI and decreases in mPAP, RAP pressures, and PVR. Reductions in PVR (to 70%) and mPAP (to 50%) and normalization of the central venous pressure are frequently detected within the first few days to weeks after PEA. Recovery of RV function occurs somewhat more slowly and frequently remains complete. An early postoperative decrease in RV function is followed by a progressive improvement of both TAPSE and right ventricular ejection fraction (RVEF) during the initial two to three years following the procedure. While the RV wall becomes thinner primarily during the first year, this process continues at a slower pace until three years after the surgery.

Interestingly, the extent of RV reverse remodeling does not depend on preoperative RV function or geometry. Results from a retrospective study that included 17 patients who had undergone PEA revealed a significant improvement in hemodynamics at day 2 [86]. Results from another study revealed similar findings although, in this case, recovery of RV function increased slowly up until six months after PEA and then stopped without achieving full recovery [87]. RV was also evaluated with cMRI and compared to results obtained with healthy controls. At four months after undergoing PEA, patients responded with significant decreases in both RV end-diastolic volume (EDV) and RV end-systolic volume (ESV) with no significant differences observed between treated patients and controls. By contrast, although both RVEFs and RV systolic volumes (SVs) increased, they did not fully normalize. The same was reported for the RV hypertrophy, including a decrease in the thickening of the RVFW that never reached the size of healthy controls. Interestingly, RVEF values correlated significantly with pre-operative disease severity and post-operative improvement, as assessed by total peripheral resistance (TPR) and decreased TPR, respectively. Early decreases in PVR and, therefore, relief of RV overload, is also an independent predictor

factor of favorable outcome after PEA [88]. The pulsatile component of the RV, afterload is also improved after PEA in association with an increase in PVC after surgery [88].

TR both before and after PEA has also been examined [89]. Results from a study cohort of 158 patients that underwent PEA revealed that the procedure resulted in a decreased prevalence of TR from 49% to 21% and that residual TR after PEA was independently associated with mortality. Residual TR was also directly associated with RA dilatation, higher RAP pressures, higher estimated sPAP, and significant comorbidities.

PEA not only results in improved RV function and RV volumes, it also alleviates RV septal bowing in left heart chambers, increases LV volumes, and improves LV function. Interventricular dyssynchrony may be normalized, thus further increasing the CO [90].

Contractility assessed by GLS and the global circumferential strain were also improved after PEA and correlated with contractility measurements determined by more invasive procedures [91]. Finally, improvement of RV-PA coupling has also been demonstrated one year after PEA [91].

Table 1 summarizes the effects of PEA on RV function.

Table 1. Evolution of right ventricular (RV) function after pulmonary endarterectomy (PEA), balloon pulmonary angioplasty (BPA), and riogicuat. cMRI = cardiac magnetic resonance imaging; CO = cardiac output; EDEI = end-diastolic eccentricity index; IVC = inferior vena cava; GLS = global longitudinal strain; RA = right atrium; RVEDAI = right ventricular end-diastolic area index; RVEDV = right ventricular end-diastolic volume; RSV = right ventricular stroke volume; RVWT = right ventricular wall thickness; TTE = transthoracic echocardiography.

Treatment	Study	Type of RV Evaluation	Parameters	Preoperative	Discharge—1 Month	3–6 Months	12 Months	24 Months
PEA	D’Armini, A.M. et al., 2007 [85]	TTE	FAC	24%	32%	33%	36%	41%
			TAPSE	15 mm	11 mm	14 mm	15 mm	16 mm
			TR grade	78%	28%	17%	23%	21%
			II/III	22 mm	17 mm	15 mm	14 mm	15 mm
			IVC	89%	14%	14%	18%	21%
			EDEI > I					
	Reesink, H.J. et al., 2007 [86]	cMRI	RVEDV	113 mL	78 mL	73 mL	74 mL	107 mL
			RVEF	30%	33%	39%	44%	46%
			RVWT	8.4 mm	7.8 mm	6.9 mm	6.3 mm	5.8 mm
	Waziri, F. et al., 2020 [91]	cMRI	RV-SV	26 mL		36 mL		
RV-EF			34%		56%			
Surie, S. et al., 2011 [92]	TTE	RV mass	49 g/m ²		29 g/m ²			
		RA area	14 cm ²			8 cm ²		
Iino, M. et al., 2008 [87]	cMRI	RVS	65 mL			71 mL		
		RVEDV	233 mL			164 mL		
Iino, M. et al., 2008 [87]	cMRI	RV mass	22 g/m ²			13 g/m ²		
		RVEF	30%			44%		
Iino, M. et al., 2008 [87]	cMRI	GLS RV	12.9%			16.5%		
		CO	3.9 L/min			5.1 L/min		
Iino, M. et al., 2008 [87]	cMRI	RV mass	22 g/m ²			13 g/m ²		
		RVEF	30%			44%		
Iino, M. et al., 2008 [87]	cMRI	GLS RV	12.9%			16.5%		
		CO	3.9 L/min			5.1 L/min		
Iino, M. et al., 2008 [87]	cMRI	RV mass	22 g/m ²			13 g/m ²		
		RVEF	30%			44%		
Iino, M. et al., 2008 [87]	cMRI	GLS RV	12.9%			16.5%		
		CO	3.9 L/min			5.1 L/min		
Iino, M. et al., 2008 [87]	cMRI	RV mass	22 g/m ²			13 g/m ²		
		RVEF	30%			44%		
Iino, M. et al., 2008 [87]	cMRI	GLS RV	12.9%			16.5%		
		CO	3.9 L/min			5.1 L/min		
Iino, M. et al., 2008 [87]	cMRI	RV mass	22 g/m ²			13 g/m ²		
		RVEF	30%			44%		
Iino, M. et al., 2008 [87]	cMRI	GLS RV	12.9%			16.5%		
		CO	3.9 L/min			5.1 L/min		
Iino, M. et al., 2008 [87]	cMRI	RV mass	22 g/m ²			13 g/m ²		
		RVEF	30%			44%		
Iino, M. et al., 2008 [87]	cMRI	GLS RV	12.9%			16.5%		
		CO	3.9 L/min			5.1 L/min		
Iino, M. et al., 2008 [87]	cMRI	RV mass	22 g/m ²			13 g/m ²		
		RVEF	30%			44%		
Iino, M. et al., 2008 [87]	cMRI	GLS RV	12.9%			16.5%		
		CO	3.9 L/min			5.1 L/min		
Iino, M. et al., 2008 [87]	cMRI	RV mass	22 g/m ²			13 g/m ²		
		RVEF	30%			44%		
Iino, M. et al., 2008 [87]	cMRI	GLS RV	12.9%			16.5%		
		CO	3.9 L/min			5.1 L/min		
Iino, M. et al., 2008 [87]	cMRI	RV mass	22 g/m ²			13 g/m ²		
		RVEF	30%			44%		
Iino, M. et al., 2008 [87]	cMRI	GLS RV	12.9%			16.5%		
		CO	3.9 L/min			5.1 L/min		
Iino, M. et al., 2008 [87]	cMRI	RV mass	22 g/m ²			13 g/m ²		
		RVEF	30%			44%		
Iino, M. et al., 2008 [87]	cMRI	GLS RV	12.9%			16.5%		
		CO	3.9 L/min			5.1 L/min		
Iino, M. et al., 2008 [87]	cMRI	RV mass	22 g/m ²			13 g/m ²		
		RVEF	30%			44%		
Iino, M. et al., 2008 [87]	cMRI	GLS RV	12.9%			16.5%		
		CO	3.9 L/min			5.1 L/min		
Iino, M. et al., 2008 [87]	cMRI	RV mass	22 g/m ²			13 g/m ²		
		RVEF	30%			44%		
Iino, M. et al., 2008 [87]	cMRI	GLS RV	12.9%			16.5%		
		CO	3.9 L/min			5.1 L/min		
Iino, M. et al., 2008 [87]	cMRI	RV mass	22 g/m ²			13 g/m ²		
		RVEF	30%			44%		
Iino, M. et al., 2008 [87]	cMRI	GLS RV	12.9%			16.5%		
		CO	3.9 L/min			5.1 L/min		
Iino, M. et al., 2008 [87]	cMRI	RV mass	22 g/m ²			13 g/m ²		
		RVEF	30%			44%		
Iino, M. et al., 2008 [87]	cMRI	GLS RV	12.9%			16.5%		
		CO	3.9 L/min			5.1 L/min		
Iino, M. et al., 2008 [87]	cMRI	RV mass	22 g/m ²			13 g/m ²		
		RVEF	30%			44%		
Iino, M. et al., 2008 [87]	cMRI	GLS RV	12.9%			16.5%		
		CO	3.9 L/min			5.1 L/min		
Iino, M. et al., 2008 [87]	cMRI	RV mass	22 g/m ²			13 g/m ²		
		RVEF	30%			44%		
Iino, M. et al., 2008 [87]	cMRI	GLS RV	12.9%			16.5%		
		CO	3.9 L/min			5.1 L/min		
Iino, M. et al., 2008 [87]	cMRI	RV mass	22 g/m ²			13 g/m ²		
		RVEF	30%			44%		
Iino, M. et al., 2008 [87]	cMRI	GLS RV	12.9%			16.5%		
		CO	3.9 L/min			5.1 L/min		
Iino, M. et al., 2008 [87]	cMRI	RV mass	22 g/m ²			13 g/m ²		
		RVEF	30%			44%		
Iino, M. et al., 2008 [87]	cMRI	GLS RV	12.9%			16.5%		
		CO	3.9 L/min			5.1 L/min		
Iino, M. et al., 2008 [87]	cMRI	RV mass	22 g/m ²			13 g/m ²		
		RVEF	30%			44%		
Iino, M. et al., 2008 [87]	cMRI	GLS RV	12.9%			16.5%		
		CO	3.9 L/min			5.1 L/min		
Iino, M. et al., 2008 [87]	cMRI	RV mass	22 g/m ²			13 g/m ²		
		RVEF	30%			44%		
Iino, M. et al., 2008 [87]	cMRI	GLS RV	12.9%			16.5%		
		CO	3.9 L/min			5.1 L/min		
Iino, M. et al., 2008 [87]	cMRI	RV mass	22 g/m ²			13 g/m ²		
		RVEF	30%			44%		
Iino, M. et al., 2008 [87]	cMRI	GLS RV	12.9%			16.5%		
		CO	3.9 L/min			5.1 L/min		
Iino, M. et al., 2008 [87]	cMRI	RV mass	22 g/m ²			13 g/m ²		
		RVEF	30%			44%		
Iino, M. et al., 2008 [87]	cMRI	GLS RV	12.9%			16.5%		
		CO	3.9 L/min			5.1 L/min		
Iino, M. et al., 2008 [87]	cMRI	RV mass	22 g/m ²			13 g/m ²		
		RVEF	30%			44%		
Iino, M. et al., 2008 [87]	cMRI	GLS RV	12.9%			16.5%		
		CO	3.9 L/min			5.1 L/min		
Iino, M. et al., 2008 [87]	cMRI	RV mass	22 g/m ²			13 g/m ²		
		RVEF	30%			44%		
Iino, M. et al., 2008 [87]	cMRI	GLS RV	12.9%			16.5%		
		CO	3.9 L/min			5.1 L/min		
Iino, M. et al., 2008 [87]	cMRI	RV mass	22 g/m ²			13 g/m ²		
		RVEF	30%			44%		
Iino, M. et al., 2008 [87]	cMRI	GLS RV	12.9%			16.5%		
		CO	3.9 L/min			5.1 L/min		
Iino, M. et al., 2008 [87]	cMRI	RV mass	22 g/m ²			13 g/m ²		
		RVEF	30%			44%		
Iino, M. et al., 2008 [87]	cMRI	GLS RV	12.9%			16.5%		
		CO	3.9 L/min			5.1 L/min		
Iino, M. et al., 2008 [87]	cMRI	RV mass	22 g/m ²			13 g/m ²		
		RVEF	30%			44%		
Iino, M. et al., 2008 [87]	cMRI	GLS RV	12.9%			16.5%		
		CO	3.9 L/min			5.1 L/min		
Iino, M. et al., 2008 [87]	cMRI	RV mass	22 g/m ²			13 g/m ²		
		RVEF	30%			44%		
Iino, M. et al., 2008 [87]	cMRI	GLS RV	12.9%			16.5%		
		CO	3.9 L/min			5.1 L/min		
Iino, M. et al., 2008 [87]	cMRI	RV mass	22 g/m ²			13 g/m ²		
		RVEF	30%			44%		
Iino, M. et al., 2008 [87]	cMRI	GLS RV	12.9%			16.5%		
		CO	3.9 L/min			5.1 L/min		
Iino, M. et al., 2008 [87]	cMRI	RV mass	22 g/m ²			13 g/m ²		
		RVEF	30%			44%		
Iino, M. et al., 2008 [87]	cMRI	GLS RV	12.9%			16.5%		
		CO	3.9 L/min			5.1 L/min		
Iino, M. et al., 2008 [87]	cMRI	RV mass	22 g/m ²			13 g/m ²		
		RVEF	30%			44%		
Iino, M. et al., 2008 [87]	cMRI	GLS RV	12.9%			16.5%		
		CO	3.9 L/min			5.1 L/min		
Iino, M. et al., 2008 [87]	cMRI	RV mass	22 g/m ²			13 g/m ²		
		RVEF	30%			44%		
Iino, M. et al., 2008 [87]	cMRI	GLS RV	12.9%			16.5%		
		CO	3.9 L/min			5.1 L/min		
Iino, M. et al., 2008 [87]	cMRI	RV mass	22 g/m ²			13 g/m ²		
		RVEF	30%			44%		
Iino, M. et al., 2008 [87]	cMRI	GLS RV	12.9%			16.5%		
		CO	3.9 L/min			5.1 L/min		
Iino, M. et al., 2008 [87]	cMRI	RV mass	22 g/m ²			13 g/m ²		
		RVEF	30%			44%		
Iino, M. et al., 2008 [87]	cMRI	GLS RV	12.9%			16.5%		
		CO	3.9 L/min			5.1 L/min		
Iino, M. et al., 2008 [87]	cMRI	RV mass	22 g/m ²			13 g/m ²		
		RVEF	30%			44%		
Iino, M. et al., 2008 [87]	cMRI	GLS RV	12.9%			16.5%		
		CO	3.9 L/min			5.1 L/min		
Iino, M. et al., 2008 [87]	cMRI	RV mass	22 g/m ²			13 g/m ²		
		RVEF	30%			44%		
Iino, M. et al., 2008 [87]	cMRI	GLS RV	12.9%			16.5%		
		CO	3.9 L/min			5.1 L/min		
Iino, M. et al., 2008 [87]	cMRI	RV mass	22 g/m ²			13 g/m ²		
		RVEF	30%			44%		
Iino, M. et al., 2008 [87]	cMRI	GLS RV	12.9%			16.5%		
		CO	3.9 L/min			5.1 L/min		
Iino, M. et al., 2008 [87]	cMRI	RV mass	22 g/m ²			13 g/m<		

Table 1. Cont.

Treatment	Study	Type of RV Evaluation	Parameters	Preoperative	Discharge—1 Month	3–6 Months	12 Months	24 Months
BPA	Fukui, S. et al., 2014 [93]	cMRI	RVSV RVEDV RV mass RVEF	41 mL/m ² 130 mL/m ² 38 g/m ² 34%		37 mL/m ² 92 mL/m ² 29 g/m ² 41%		
	Broch, K. et al., 2016 [94]	TTE	RV basal diameter RVWT FAC RA area TAPSE S' RV free wall strain	50 mm 6.5 mm 26% 26.5 cm ² 19 mm 8.9 cm/s −17%		46 mm 5.6 mm 32% 22.7 cm ² 22 mm 10 cm/s −21.7%		
	Tsugu, T. et al., 2015 [95]	TTE	RV basal diameter RVEDV RVSV FAC RVEF TAPSE S' RV mid free wall strain	33.7 mm 76.4 mL/m ² 28.6 mL/m ² 22.6% 38% 17.8 mm 11.1 cm/s −19.2%	30.7 mm 64 mL/m ² 29.9 mL/m ²			
	Sato, H. et al., 2016 [96]	cMRI	RVSV RVEDV RV mass RVEF	40 mL/m ² 104 mL/m ² 33.5 g/m ² 41%	43 mL/m ² 85 mL/m ² 26.4 g/m ² 51%			
	Yamasaki, Y. et al., 2017 [97]	cMRI	RVSV RVEDV RVEF	38.4 mL/m ² 118 mL/m ² 35.5%		40.5 mL/m ² 33.5 g/m ² 42.4%		
	Schoenfeld, C. et al., 2019 [98]	cMRI	RVSV RVEDV RV mass RVEF	43 mL/m ² 90 mL/m ² 35 g/m ² 51%		44 mL/m ² 90 mL/m ² 36 g/m ² 51%		
	Marra, A.M. et al., 2015 [99]	TTE	LV eccentricity index RA area TAPSE S' RVWT IVC	1.2 25 cm ² 19.5 mm 11 cm/s 9.5 mm 17 mm		0.95 21 cm ² 21.5 mm 12 cm/s 8.3 mm 16.8 mm	1 19.5 cm ² 23 mm 13 cm/s 8 mm 15.6 mm	
Riociguat	Murata, M. et al., 2018 [100]	TTE	RV basal diameter RVFAC TAPSE S' RV GLS IVC	39 mm 35.6 cm ² 17.5 mm 10.7 cm/s −13.9% 15 mm		36 mm 39.6 cm ² 18.1 mm 11.4 cm/s −17.4% 13.8 mm		

Table 1. Cont.

Treatment	Study	Type of RV Evaluation	Parameters	Preoperative	Discharge—1 Month	3–6 Months	12 Months	24 Months
	Murata, M. et al., 2021 [101]	TTE	RV basal diameter	39.5 mm			36.5 mm	
			RV-EDAI	13.5 cm ²			11.9 cm ²	
			RV FAC	33 cm ²			38 cm ²	
			TAPSE	18 mm			19 mm	
			S'	10.6 cm/s			11.7 cm/s	
			RV GLS	−13.9%			−17.6%	
			RV dyssynchrony index	105 ms			78 ms	
			IVC	9.1 mm			9.8 mm	

4.2. Incomplete Restoration of RV Function

A non-invasive assessment of RV function with TAPSE, RV-S, and RV-MPI documents the incomplete restoration of RV function one year after PEA despite normalization of RV geometry and after a transient depression observed in the early postoperative period [92]. RV wall stress improves after surgery but frequently remains higher than levels detected in healthy subjects. Similar findings were reported in a study focused on RV diastolic function evaluated by echocardiography (i.e., RV E/E') [92]. Other parameters, including RV mass assessed by cMRI, decrease but do not undergo complete restoration to the pre-disease state. In the early postoperative phase, only a poor correlation was reported between TAPSE and hemodynamic recovery, in contrast to the stronger associations reported for the pre-operative setting. A higher correlation was reported for the RV to LV end-diastolic area ratio. These findings underscore the need for a careful interpretation of the echocardiographic parameters describing RV function in the first several days after PEA that do not predict hemodynamic improvement [102]. This partial restoration of RV function suggests that increased RV afterload may persist and/or an RV plasticity is incomplete, thus precluding its return to a fully restored state. Incomplete improvement in RV function was correlated to exercise limitation [103] and with abnormal hemodynamic responses observed during exercise and an increased mPAP/CO slope despite normalization (or near normalization) of PAP [104].

Incomplete restoration of RV function and RV mass has been linked to evidence of residual PH after PEA [105]. Up to one-third of patients may have persistent (or residual) PH despite an otherwise successful PEA procedure. Persistent PH and poor outcomes can result from incomplete removal of more distal thrombi and/or from concomitant small-vessel disease in patients with the surgically-amenable proximal disease. Changes in PVC after PEA have also been evaluated [39]. In these cases, the absence of improvement has been correlated with poor functional status [103]. Patients presenting with normal hemodynamic parameters at rest after PEA may experience an abnormal increase in PVR and a decrease in PVC during exercise, which have been significantly associated with exercise limitation [57]. Likewise, abnormal resistive and pulsatile pulmonary vascular function after PEA have been associated with a higher mPAP/CO slope [104]; these conditions may respond to the administration of sildenafil. Other parameters of concern include the detection of a systolic notch in the pulmonary artery flow, which suggests the persistence of an early wave flow reflection [106]. This finding has been associated with poor outcomes after PEA [107].

Other explanations that have been proposed to explain the incomplete restoration of RV function after PEA involve the development of myocardial fibrosis and thus intrinsic decreased contractility. Similarly, RVSV also improved after PEA, albeit without a complete restoration to levels exhibited by healthy subjects [108]. Moreover, improvements in these parameters with exercise were also limited and correlated with symptoms. A recent cMRI

study of 22 CTEPH patients that was designed to assess regional myocardial function after PEA revealed substantial heterogeneity with respect to recovery of peak systolic longitudinal (i.e., no improvement at 12 days after PEA), radial, and circumferential strain (i.e., improvement at 12 days after PEA) in both ventricles by tissue-tracking analysis despite significant improvements in mPAP [109]. These findings suggest the possibility of differential timing of recovery for different types of myocardial fibers according to their relative overload and may also explain the progressive restoration of RV function after PEA. Figure 3 summarizes the evolution of RV structure and function after PEA.

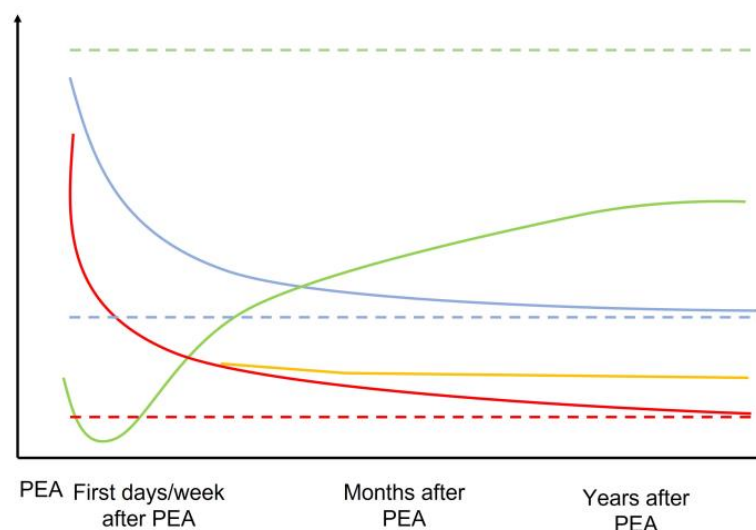


Figure 3. Schematic representation of the evolution of the mPAP, RV geometry, and RV function across time after PEA. The dotted line represents the normal expected values for each parameter. Green = RV function. Blue = RV geometry and dilatation. Red = mPAP if normalized. Orange = mPAP if residual PH after PEA. Dotted lines represent normal situations.

4.3. Effect of Balloon Pulmonary Angioplasty on RV Function

Balloon pulmonary angioplasty (BPA) is an established modality used to treat CTEPH patients [1,2]. BPA is indicated for symptomatic patients who are unable to undergo PEA because of distal disease, persistent/recurrent PH after surgery, or other comorbidities. BPA has been associated with improvements in hemodynamics, exercise capacity, serum levels of N-terminal (NT) pro-brain natriuretic peptide (BNP), and RV function [93,110,111]. Because BPA was developed more recently than PEA, there is only limited evidence available in support of BPA-mediated improvement of right heart function. However, given that both techniques share mechanical aims (i.e., the removal of macroscopic obstruction in the pulmonary vascular bed) [112], the knowledge that has accumulated for PEA may also support the efficacy of BPA in these circumstances.

Results from multiple studies have revealed improvements in hemodynamics together with improvements in both cardiac function and RV afterload via increases in CO and decreases in mPAP and PVR [110,111,113]. Hemodynamic improvements monitored by invasive methods can be translated into improvements in both RV function and geometry [94,95]. In one retrospective study, 30 CTEPH patients who could not undergo surgery were treated with BPA and then followed with cMRI [96]. Improvements were reported in all RV parameters that were assessed by cMRI, except RVSV index. PA flow rate and area were also evaluated in 22 patients; the results of this study revealed increases in average velocity and significant decreases in area, respectively. Similar results were reported from another prospective study, in which 20 patients exhibited decreased RV volumes and improvements in RVEF when evaluated with cMRI [97]. Moreover, the authors reported improvements in interventricular dyssynchrony as assessed by the time to peak of the circumferential strain. Another cMRI study of 29 patients who were evaluated two months

after BPA revealed increased pulmonary perfusion, RVEF, RVSV, CO, ventricular mass index, and serum NT-proBNP levels [98]. Another study that included 45 consecutive patients diagnosed with CTEPH revealed significant reverse remodeling of the right heart chambers and improvements in RVFW strain [114]. Interestingly, additional improvements were reported in patients with residual PH after PEA. Speckle tracking parameters, including RVFW longitudinal strain, the RV peak systolic strain dispersion index, and the time to peak longitudinal systolic strain differences also underwent significant improvement after BPA, although they did not reach values reported for healthy subjects [115]. A recent meta-analysis that included 10 studies and 299 patients focused on an evaluation of RV function by cMRI or echocardiography revealed improvements in RV function after BPA, specifically increases in RVEF and decreased RV volumes [116]. While improvements in PVC have not been fully evaluated in patients undergoing BPA, one recent study demonstrated improvements in pulsatile RV afterload of the RV assessed by PVC [113].

4.4. Medical Therapy and RV Function

While PEA remains the treatment of choice for CTEPH with a proximal disease, approximately 40% of the patients are considered inoperable secondary to inaccessible vascular obstruction or significant comorbidities [34]. Riociguat, a first-in-class stimulator of sGC, is the only medication that is currently approved for inoperable CTEPH patients or those with persistent/recurrent PH after PEA [11]. Riociguat sensitizes sGC to endogenous nitric oxide (NO) and also directly stimulates sGC independently of NO. Riociguat-mediated activation of sGC results in increased production of cGMP which promotes vasodilation and inhibition of pulmonary vascular remodeling.

Administration of riociguat resulted in improved RV function, reversal of RV hypertrophy, improved vascular remodeling, and decreased myocardial fibrosis in various animal models of PH [117–120].

Results from a human clinical study revealed that the administration of riociguat results in improved pulmonary hemodynamics associated with improvements in mPAP, CO, CI, and PVR. The changes observed in PVR correlated with increased exercise capacity [121] and remained effective for two years [122]. Interestingly, the administration of riociguat also resulted in decreased systemic vascular resistance in patients diagnosed with CTEPH. This finding explains the hypotension frequently exhibited by patients on this treatment regimen and may contribute to an increase in CO. Moreover, riociguat treatment can reverse the observed enlargement of the right heart chambers (RV and RA), improve TAPSE, RV S', RV FAC, and RV remodeling as assessed by RV wall thickness through one year after the initiation of therapy [99,123]. RV-GLS was also reduced in CTEPH patients who had undergone treatment with riociguat [100], including those with mild PH after PEA or BPA [101]; these results suggest a mechanism that includes pharmacological recruitment of RV contractile reserve. A recent study of riociguat treatment after BPA demonstrated the beneficial impact of this drug in subjects with mPAP < 30 mmHg. They exhibited improvements in resting PVR and CO and a decrease in the mPAP/CO ratio during exercise [124]. Interestingly, riociguat also had a positive impact on hemodynamics in CTEPH patients that had previously undergone treatment with sildenafil [125]. A recent crossover study that compared BPA and riociguat treatment revealed that BPA was more efficient at decreasing mPAP while riociguat was more effective at improving CO; these results suggested that these modalities target different pathways and elicit different effects [126]. However, no studies have assessed the role of riociguat and its withdrawal after BPA for patients with normalized hemodynamic parameters.

5. Conclusions

RV function is an important marker of prognosis in patients diagnosed with CTEPH. The physiopathology of RV dysfunction in this potentially severe disease is complex and involves a multifactorial increase in RV afterload that may be assessed non-invasively by echocardiography and cMRI. Invasive procedures, such as PEA and BPA, may be used

to normalize hemodynamics and RV geometry in patients with this disease. However, the observed decrease in afterload does not systematically translate into a normalization of RV function. Persistent RV dysfunction may be linked to ongoing RV overload due to residual obstruction or microvasculopathy. Persistent dysfunction may also be due to diminished levels of intrinsic RV contractility potentially associated with irreversible myocardial fibrosis. Administration of the sGC-activating drug, riociguat, results in improved RV function and may contribute to the ongoing amelioration of RV function after surgery or other interventional treatments.

Author Contributions: Conceptualization, S.M., M.D., L.G.; methodology S.M., L.G.; validation: S.M., T.V., G.C., R.Q., M.D., L.G.; writing: S.M., T.V., R.Q., L.G.; All authors have read and agreed to the published version of the manuscript.

Funding: This research received no external funding.

Institutional Review Board Statement: Not applicable.

Informed Consent Statement: Not applicable.

Data Availability Statement: Not applicable.

Conflicts of Interest: M.D. and L.G. received consultancy fees and travel fees from MSD and Janssen.

References

- Humbert, M.; Kovacs, G.; Hoeper, M.M.; Badagliacca, R.; Berger, R.M.; Brida, M.; Carlsen, J.; Coats, A.J.; Escribano-Subias, P.; Ferrari, P.; et al. 2022 ESC/ERS Guidelines for the diagnosis and treatment of pulmonary hypertension. *Eur. Respir. J.* **2022**, *43*, 3618–3731.
- Delcroix, M.; Torbicki, A.; Gopalan, D.; Sitbon, O.; Klok, F.A.; Lang, I.; Jenkins, D.; Kim, N.H.; Humbert, M.; Jais, X.; et al. ERS statement on chronic thromboembolic pulmonary hypertension. *Eur. Respir. J.* **2020**, *57*, 2002828. [[CrossRef](#)] [[PubMed](#)]
- Fauché, A.; Presles, E.; Sanchez, O.; Jais, X.; Le Mao, R.; Robin, P.; Pernod, G.; Bertoletti, L.; Jegou, P.; Parent, F.; et al. Frequency and Predictors for Chronic Thromboembolic Pulmonary Hypertension after a First Unprovoked Pulmonary Embolism: Results from PADIS studies. *J. Thromb. Haemost.* **2022**, *20*, 2850–2861. [[CrossRef](#)]
- Valerio, L.; Mavromanolis, A.C.; Barco, S.; Abele, C.; Becker, D.; Bruch, L.; Ewert, R.; Faehling, M.; Fistera, D.; Gerhardt, F.; et al. Chronic thromboembolic pulmonary hypertension and impairment after pulmonary embolism: The FOCUS study. *Eur. Heart J.* **2022**, *43*, 3387–3398. [[CrossRef](#)]
- Simonneau, G.; Torbicki, A.; Dorfmüller, P.; Kim, N. The pathophysiology of chronic thromboembolic pulmonary hypertension. *Eur. Respir. Rev.* **2017**, *26*, 160112. [[CrossRef](#)]
- Ruaro, B.; Baratella, E.; Caforio, G.; Confalonieri, P.; Wade, B.; Marrocchio, C.; Geri, P.; Pozzan, R.; Andrisano, A.G.; Cova, M.A.; et al. Chronic Thromboembolic Pulmonary Hypertension: An Update. *Diagnostics* **2022**, *12*, 235. [[CrossRef](#)]
- Dorfmüller, P.; Günther, S.; Ghigna, M.-R.; De Montpréville, V.T.; Boulate, D.; Paul, J.-F.; Jais, X.; Decante, B.; Simonneau, G.; Darteville, P.; et al. Microvascular disease in chronic thromboembolic pulmonary hypertension: A role for pulmonary veins and systemic vasculature. *Eur. Respir. J.* **2014**, *44*, 1275–1288. [[CrossRef](#)]
- Simonneau, G.; Dorfmüller, P.; Guignabert, C.; Mercier, O.; Humbert, M. Chronic thromboembolic pulmonary hypertension: The magic of pathophysiology. *Ann. Cardiothorac. Surg.* **2022**, *11*, 106–119. [[CrossRef](#)]
- Verbelen, T.; Godinas, L.; Maleux, G.; Coolen, J.; Claessen, G.; Belge, C.; Meyns, B.; Delcroix, M. Chronic thromboembolic pulmonary hypertension: Diagnosis, operability assessment and patient selection for pulmonary endarterectomy. *Ann. Cardiothorac. Surg.* **2022**, *11*, 82–97. [[CrossRef](#)]
- Kim, N.H.; Delcroix, M.; Jenkins, D.P.; Channick, R.; Darteville, P.; Jansa, P.; Lang, I.; Madani, M.M.; Ogino, H.; Pengo, V.; et al. Chronic thromboembolic pulmonary hypertension. *Eur. Respir. J.* **2019**, *53*, 1801915. [[CrossRef](#)]
- Ghofrani, H.-A.; D’Armini, A.M.; Grimminger, F.; Hoeper, M.M.; Jansa, P.; Kim, N.H.; Mayer, E.; Simonneau, G.; Wilkins, M.R.; Fritsch, A.; et al. Riociguat for the treatment of chronic thromboembolic pulmonary hypertension. *N. Engl. J. Med.* **2013**, *369*, 319–329. [[CrossRef](#)] [[PubMed](#)]
- Hoeper, M.M.; Madani, M.M.; Nakanishi, N.; Meyer, B.; Cebotari, S.; Rubin, L.J. Chronic thromboembolic pulmonary hypertension. *Lancet Respir. Med.* **2014**, *2*, 573–582. [[CrossRef](#)] [[PubMed](#)]
- Lankhaar, J.-W.; Westerhof, N.; Faes, T.J.C.; Marques, K.M.J.; Marcus, J.T.; Postmus, P.E.; Vonk-Noordegraaf, A. Quantification of right ventricular afterload in patients with and without pulmonary hypertension. *Am. J. Physiol. Circ. Physiol.* **2006**, *291*, H1731–H1737. [[CrossRef](#)] [[PubMed](#)]
- Nakayama, Y.; Nakanishi, N.; Sugimachi, M.; Takaki, H.; Kyotani, S.; Satoh, T.; Okano, Y.; Kunieda, T.; Sunagawa, K. Characteristics of pulmonary artery pressure waveform for differential diagnosis of chronic pulmonary thromboembolism and primary pulmonary hypertension. *J. Am. Coll. Cardiol.* **1997**, *29*, 1311–1316. [[CrossRef](#)] [[PubMed](#)]

15. Nakayama, Y.; Sugimachi, M.; Nakanishi, N.; Takaki, H.; Okano, Y.; Satoh, T.; Miyatake, K.; Sunagawa, K. Noninvasive differential diagnosis between chronic pulmonary thromboembolism and primary pulmonary hypertension by means of Doppler ultrasound measurement. *J. Am. Coll. Cardiol.* **1998**, *31*, 1367–1371. [[CrossRef](#)]
16. Nakayama, Y.; Nakanishi, N.; Hayashi, T.; Nagaya, N.; Sakamaki, F.; Satoh, N.; Ohya, H.; Kyotani, S. Pulmonary artery reflection for differentially diagnosing primary pulmonary hypertension and chronic pulmonary thromboembolism. *J. Am. Coll. Cardiol.* **2001**, *38*, 214–218. [[CrossRef](#)]
17. Fukumitsu, M.; Groeneveldt, J.A.; Braams, N.J.; Bayoumy, A.A.; Marcus, J.T.; Meijboom, L.J.; de Man, F.S.; Bogaard, H.; Noordegraaf, A.V.; Westerhof, B.E. When right ventricular pressure meets volume: The impact of arrival time of reflected waves on right ventricle load in pulmonary arterial hypertension. *J. Physiol.* **2022**, *600*, 2327–2344. [[CrossRef](#)]
18. Castelain, V.; Hervé, P.; Lecarpentier, Y.; Duroux, P.; Simonneau, G.; Chemla, D. Pulmonary artery pulse pressure and wave reflection in chronic pulmonary thromboembolism and primary pulmonary hypertension. *J. Am. Coll. Cardiol.* **2001**, *37*, 1085–1092. [[CrossRef](#)]
19. Pagnamenta, A.; Vanderpool, R.; Brimiouille, S.; Naeije, R. Proximal pulmonary arterial obstruction decreases the time constant of the pulmonary circulation and increases right ventricular afterload. *J. Appl. Physiol.* **2013**, *114*, 1586–1592. [[CrossRef](#)]
20. Saouti, N.; Westerhof, N.; Helderma, F.; Marcus, J.T.; Stergiopulos, N.; Westerhof, B.E.; Boonstra, A.; Postmus, P.E.; Vonk-Noordegraaf, A. RC time constant of single lung equals that of both lungs together: A study in chronic thromboembolic pulmonary hypertension. *Am. J. Physiol. Heart Circ. Physiol.* **2009**, *297*, H2154–H2160. [[CrossRef](#)]
21. Naeije, R.; Delcroix, M. Is the time constant of the pulmonary circulation truly constant? *Eur. Respir. J.* **2014**, *43*, 1541–1542. [[CrossRef](#)] [[PubMed](#)]
22. Moser, K.M.; Bloor, C.M. Pulmonary vascular lesions occurring in patients with chronic major vessel thromboembolic pulmonary hypertension. *Chest* **1993**, *103*, 685–692. [[CrossRef](#)] [[PubMed](#)]
23. Kapitan, K.S.; Buchbinder, M.; Wagner, P.D.; Moser, K.M. Mechanisms of hypoxemia in chronic thromboembolic pulmonary hypertension. *Am. Rev. Respir. Dis.* **1989**, *139*, 1149–1154. [[CrossRef](#)]
24. Boulate, D.; Perros, F.; Dorfmüller, P.; Arthur-Ataam, J.; Guihaire, J.; Lamrani, L.; Decante, B.; Humbert, M.; Eddahibi, S.; Darteville, P.; et al. Pulmonary microvascular lesions regress in reperfused chronic thromboembolic pulmonary hypertension. *J. Heart Lung Transplant.* **2015**, *34*, 457–467. [[CrossRef](#)] [[PubMed](#)]
25. Quarck, R.; Wynants, M.; Verbeken, E.; Meyns, B.; Delcroix, M. Contribution of inflammation and impaired angiogenesis to the pathobiology of chronic thromboembolic pulmonary hypertension. *Eur. Respir. J.* **2015**, *46*, 431–443. [[CrossRef](#)] [[PubMed](#)]
26. Gerges, C.; Gerges, M.; Friewald, R.; Fesler, P.; Dorfmüller, P.; Sharma, S.; Karlocai, K.; Skoro-Sajer, N.; Jakowitsch, J.; Moser, B.; et al. Microvascular Disease in Chronic Thromboembolic Pulmonary Hypertension: Hemodynamic Phenotyping and Histomorphometric Assessment. *Circulation* **2020**, *141*, 376–386. [[CrossRef](#)]
27. Braams, N.J.; van Leeuwen, J.W.; Noordegraaf, A.V.; Nossent, E.J.; Ruigrok, D.; Marcus, J.T.; Bogaard, H.J.; Meijboom, L.J.; de Man, F.S. Right ventricular adaptation to pressure-overload: Differences between chronic thromboembolic pulmonary hypertension and idiopathic pulmonary arterial hypertension. *J. Heart Lung Transplant.* **2021**, *40*, 458–466. [[CrossRef](#)]
28. Vonk-Noordegraaf, A.; Haddad, F.; Chin, K.M.; Forfia, P.R.; Kawut, S.M.; Lumens, J.; Naeije, R.; Newman, J.; Oudiz, R.J.; Provencher, S.; et al. Right heart adaptation to pulmonary arterial hypertension: Physiology and pathobiology. *J. Am. Coll. Cardiol.* **2013**, *62* (Suppl. 25), D22–D33. [[CrossRef](#)]
29. Sanz, J.; Sánchez-Quintana, D.; Bossone, E.; Bogaard, H.J.; Naeije, R. Anatomy, Function, and Dysfunction of the Right Ventricle: JACC State-of-the-Art Review. *J. Am. Coll. Cardiol.* **2019**, *73*, 1463–1482. [[CrossRef](#)] [[PubMed](#)]
30. Vonk-Noordegraaf, A.; Westerhof, B.E.; Westerhof, N. The Relationship Between the Right Ventricle and its Load in Pulmonary Hypertension. *J. Am. Coll. Cardiol.* **2017**, *69*, 236–243. [[CrossRef](#)]
31. Poels, E.M.; da Costa Martins, P.A.; van Empel, V.P.M. Adaptive capacity of the right ventricle: Why does it fail? *Am. J. Physiol. Heart Circ. Physiol.* **2015**, *308*, H803–H813. [[CrossRef](#)] [[PubMed](#)]
32. Leopold, J.A.; Kawut, S.M.; Aldred, M.A.; Archer, S.L.; Benza, R.L.; Bristow, M.R.; Brittain, E.L.; Chesler, N.; DeMan, F.S.; Erzurum, S.C.; et al. Diagnosis and Treatment of Right Heart Failure in Pulmonary Vascular Diseases: A National Heart, Lung, and Blood Institute Workshop. *Circ. Heart Fail.* **2021**, *14*, e007975. [[CrossRef](#)] [[PubMed](#)]
33. Gurudevan, S.V.; Malouf, P.J.; Auger, W.R.; Waltman, T.J.; Madani, M.; Raisinghani, A.B.; DeMaria, A.N.; Blanchard, D.G. Abnormal Left Ventricular Diastolic Filling in Chronic Thromboembolic Pulmonary Hypertension. *J. Am. Coll. Cardiol.* **2007**, *49*, 1334–1339. [[CrossRef](#)] [[PubMed](#)]
34. Yamagata, Y.; Ikeda, S.; Kojima, S.; Ueno, Y.; Nakata, T.; Koga, S.; Ohno, C.; Yonekura, T.; Yoshimuta, T.; Minami, T.; et al. Right Ventricular Dyssynchrony in Patients With Chronic Thromboembolic Pulmonary Hypertension and Pulmonary Arterial Hypertension. *Circ. J.* **2022**, *86*, 936–944. [[CrossRef](#)] [[PubMed](#)]
35. Trip, P.; Rain, S.; Handoko, M.L.; Van Der Bruggen, C.; Bogaard, H.J.; Marcus, J.T.; Boonstra, A.; Westerhof, N.; Vonk-Noordegraaf, A.; De Man, F.S. Clinical relevance of right ventricular diastolic stiffness in pulmonary hypertension. *Eur. Respir. J.* **2015**, *45*, 1603–1612. [[CrossRef](#)]
36. Rain, S.; Andersen, S.; Najafi, A.; Gammelgaard Schultz, J.; da Silva Gonçalves Bós, D.; Handoko, M.L.; Bogaard, H.J.; Vonk-Noordegraaf, A.; Andersen, A.; Van Der Velden, J.; et al. Right Ventricular Myocardial Stiffness in Experimental Pulmonary Arterial Hypertension: Relative Contribution of Fibrosis and Myofibril Stiffness. *Circ. Heart Fail.* **2016**, *9*, e002636. [[CrossRef](#)]

37. van Wolferen, S.A.; Marcus, J.T.; Westerhof, N.; Spreeuwenberg, M.D.; Marques, K.M.; Bronzwaer, J.G.; Henkens, I.R.; Gan, C.T.J.; Boonstra, A.; Postmus, P.E.; et al. Right coronary artery flow impairment in patients with pulmonary hypertension. *Eur. Heart J.* **2008**, *29*, 120–127. [[CrossRef](#)]
38. Boulate, D.; Ataam, J.A.; Connolly, A.J.; Giraldeau, G.; Amsallem, M.; Decante, B.; Lamrani, L.; Fadel, E.; Dorfmüller, P.; Perros, F.; et al. Early Development of Right Ventricular Ischemic Lesions in a Novel Large Animal Model of Acute Right Heart Failure in Chronic Thromboembolic Pulmonary Hypertension. *J. Card. Fail.* **2017**, *23*, 876–886. [[CrossRef](#)]
39. Nishizaki, M.; Ogawa, A.; Matsubara, H. High Right Ventricular Afterload during Exercise in Patients with Pulmonary Arterial Hypertension. *J. Clin. Med.* **2021**, *10*, 2024. [[CrossRef](#)]
40. Spruijt, O.A.; de Man, F.S.; Groepenhoff, H.; Oosterveer, F.; Westerhof, N.; Vonk-Noordegraaf, A.; Bogaard, H.-J. The effects of exercise on right ventricular contractility and right ventricular-arterial coupling in pulmonary hypertension. *Am. J. Respir. Crit. Care Med.* **2015**, *191*, 1050–1057. [[CrossRef](#)]
41. Natarajan, R.; Drake, J.I.; Bogaard, H.J.; Fawcett, P.M.; Clifton, B.; Gao, Y.; Voelkel, N.F. Molecular signature of a right heart failure program in chronic severe pulmonary hypertension. *Am. J. Respir. Cell Mol. Biol.* **2011**, *45*, 1239–1247.
42. Sutendra, G.; Dromparis, P.; Paulin, R.; Zervopoulos, S.; Haromy, A.; Nagendran, J.; Michelakis, E.D. A metabolic remodeling in right ventricular hypertrophy is associated with decreased angiogenesis and a transition from a compensated to a decompensated state in pulmonary hypertension. *J. Mol. Med.* **2013**, *91*, 1315–1327. [[CrossRef](#)] [[PubMed](#)]
43. Bär, H.; Kreuzer, J.; Cojoc, A.; Jahn, L. Upregulation of embryonic transcription factors in right ventricular hypertrophy. *Basic Res. Cardiol.* **2003**, *98*, 285–294. [[CrossRef](#)] [[PubMed](#)]
44. Lemay, S.-E.; Awada, C.; Shimauchi, T.; Wu, W.-H.; Bonnet, S.; Provencher, S.; Boucherat, O. Fetal Gene Reactivation in Pulmonary Arterial Hypertension: GOOD, BAD, or BOTH? *Cells* **2021**, *10*, 1473. [[CrossRef](#)] [[PubMed](#)]
45. Dewachter, C.; Belhaj, A.; Rondelet, B.; Vercruyssen, M.; Schraufnagel, D.P.; Rimmelink, M.; Brimiouille, S.; Kerbaul, F.; Naeije, R.; Dewachter, L. Myocardial inflammation in experimental acute right ventricular failure: Effects of prostacyclin therapy. *J. Heart Lung Transplant.* **2015**, *34*, 1334–1345. [[CrossRef](#)]
46. Sun, X.Q.; Abbate, A.; Bogaard, H.J. Role of cardiac inflammation in right ventricular failure. *Cardiovasc. Res.* **2017**, *113*, 1441–1452. [[CrossRef](#)]
47. de Man, F.S.; Tu, L.; Handoko, M.L.; Rain, S.; Ruiter, G.; François, C.; Schalij, I.; Dorfmüller, P.; Simonneau, G.; Fadel, E.; et al. Dysregulated renin-angiotensin-aldosterone system contributes to pulmonary arterial hypertension. *Am. J. Respir. Crit. Care Med.* **2012**, *186*, 780–789. [[CrossRef](#)]
48. Archer, S.L.; Fang, Y.H.; Ryan, J.J.; Piao, L. Metabolism and bioenergetics in the right ventricle and pulmonary vasculature in pulmonary hypertension. *Pulm. Circ.* **2013**, *3*, 144–152. [[CrossRef](#)]
49. Roller, F.C.; Wiedenroth, C.; Breithecker, A.; Liebetau, C.; Mayer, E.; Schneider, C.; Rolf, A.; Hamm, C.; Krombach, G.A. Native T1 mapping and extracellular volume fraction measurement for assessment of right ventricular insertion point and septal fibrosis in chronic thromboembolic pulmonary hypertension. *Eur. Radiol.* **2017**, *27*, 1980–1991. [[CrossRef](#)]
50. Roller, F.C.; Kriechbaum, S.; Breithecker, A.; Liebetau, C.; Haas, M.; Schneider, C.; Rolf, A.; Guth, S.; Mayer, E.; Hamm, C.; et al. Correlation of native T1 mapping with right ventricular function and pulmonary haemodynamics in patients with chronic thromboembolic pulmonary hypertension before and after balloon pulmonary angioplasty. *Eur. Radiol.* **2019**, *29*, 1565–1573. [[CrossRef](#)]
51. Suen, C.M.; Chaudhary, K.R.; Deng, Y.; Jiang, B.; Stewart, D.J. Fischer rats exhibit maladaptive structural and molecular right ventricular remodelling in severe pulmonary hypertension: A genetically prone model for right heart failure. *Cardiovasc. Res.* **2019**, *115*, 788–799. [[CrossRef](#)]
52. Noly, P.-E.; Haddad, F.; Arthur-Ataam, J.; Langer, N.; Dorfmüller, P.; Loisel, F.; Guihaire, J.; Decante, B.; Lamrani, L.; Fadel, E.; et al. The importance of capillary density-stroke work mismatch for right ventricular adaptation to chronic pressure overload. *J. Thorac. Cardiovasc. Surg.* **2017**, *154*, 2070–2079. [[CrossRef](#)] [[PubMed](#)]
53. Potus, F.; Ruffenach, G.; Dahou, A.; Thebault, C.; Breuils-Bonnet, S.; Tremblay, È.; Nadeau, V.; Paradis, R.; Graydon, C.; Wong, R.; et al. Downregulation of MicroRNA-126 Contributes to the Failing Right Ventricle in Pulmonary Arterial Hypertension. *Circulation* **2015**, *132*, 932–943. [[CrossRef](#)] [[PubMed](#)]
54. Kojonazarov, B.; Novoyatleva, T.; Boehm, M.; Happe, C.; Sibinska, Z.; Tian, X.; Sajjad, A.; Luitel, H.; Kriechling, P.; Posern, G.; et al. p38 MAPK Inhibition Improves Heart Function in Pressure-Loaded Right Ventricular Hypertrophy. *Am. J. Respir. Cell Mol. Biol.* **2017**, *57*, 603–614. [[CrossRef](#)] [[PubMed](#)]
55. Gomez-Arroyo, J.; Sakagami, M.; Syed, A.A.; Farkas, L.; Van Tassell, B.; Kraskauskas, D.; Mizuno, S.; Abbate, A.; Bogaard, H.J.; Byron, P.R.; et al. Iloprost reverses established fibrosis in experimental right ventricular failure. *Eur. Respir. J.* **2015**, *45*, 449–462. [[CrossRef](#)] [[PubMed](#)]
56. Mehta, B.B.; Auger, D.A.; Gonzalez, J.A.; Workman, V.; Chen, X.; Chow, K.; Stump, C.J.; Mazimba, S.; Kennedy, J.L.W.; Gay, E.; et al. Detection of elevated right ventricular extracellular volume in pulmonary hypertension using Accelerated and Navigator-Gated Look-Locker Imaging for Cardiac T1 Estimation (ANGIE) cardiovascular magnetic resonance. *J. Cardiovasc. Magn. Reson.* **2015**, *17*, 110. [[CrossRef](#)]
57. Bonderman, D.; Martischnig, A.M.; Vonbank, K.; Nikfardjam, M.; Meyer, B.; Heinz, G.; Klepetko, W.; Naeije, R.; Lang, I.M. Right ventricular load at exercise is a cause of persistent exercise limitation in patients with normal resting pulmonary vascular resistance after pulmonary endarterectomy. *Chest* **2011**, *139*, 122–127. [[CrossRef](#)]

58. de Perrot, M.; McRae, K.; Shargall, Y.; Thenganatt, J.; Moric, J.; Mak, S.; Granton, J.T. Early postoperative pulmonary vascular compliance predicts outcome after pulmonary endarterectomy for chronic thromboembolic pulmonary hypertension. *Chest* **2011**, *140*, 34–41. [[CrossRef](#)]
59. Claeys, M.; Claessen, G.; La Gerche, A.; Petit, T.; Belge, C.; Meyns, B.; Bogaert, J.; Willems, R.; Claus, P.; Delcroix, M. Impaired Cardiac Reserve and Abnormal Vascular Load Limit Exercise Capacity in Chronic Thromboembolic Disease. *JACC Cardiovasc. Imaging* **2019**, *12 Pt 1*, 1444–1456. [[CrossRef](#)]
60. Blumberg, F.C.; Arzt, M.; Lange, T.; Schroll, S.; Pfeifer, M.; Wensel, R. Impact of right ventricular reserve on exercise capacity and survival in patients with pulmonary hypertension. *Eur. J. Heart Fail.* **2013**, *15*, 771–775. [[CrossRef](#)]
61. Kamimura, Y.; Okumura, N.; Adachi, S.; Shimokata, S.; Tajima, F.; Nakano, Y.; Hirashiki, A.; Murohara, T.; Kondo, T. Usefulness of scoring right ventricular function for assessment of prognostic factors in patients with chronic thromboembolic pulmonary hypertension. *Heart Vessels* **2018**, *33*, 1220–1228. [[CrossRef](#)] [[PubMed](#)]
62. Godinas, L.; Sattler, C.; Lau, E.; Jais, X.; Taniguchi, Y.; Jevnikar, M.; Weatherald, J.; Sitbon, O.; Savale, L.; Montani, D.; et al. Dead-space ventilation is linked to exercise capacity and survival in distal chronic thromboembolic pulmonary hypertension. *J. Heart Lung Transplant.* **2017**, *36*, 1234–1242. [[CrossRef](#)] [[PubMed](#)]
63. Howden, E.J.; Ruiz-Carmona, S.; Claeys, M.; De Bosscher, R.; Willems, R.; Meyns, B.; Verbelen, T.; Maleux, G.; Godinas, L.; Belge, C.; et al. Oxygen Pathway Limitations in Patients with Chronic Thromboembolic Pulmonary Hypertension. *Circulation* **2021**, *143*, 2061–2073. [[CrossRef](#)] [[PubMed](#)]
64. Delcroix, M.; Lang, I.; Pepke-Zaba, J.; Jansa, P.; D’Armini, A.M.; Snijder, R.; Bresser, P.; Torbicki, A.; Mellekjaer, S.; Lewczuk, J.; et al. Long-Term Outcome of Patients With Chronic Thromboembolic Pulmonary Hypertension: Results From an International Prospective Registry. *Circulation* **2016**, *133*, 859–871. [[CrossRef](#)]
65. Jamieson, S.W.; Kapelanski, D.P.; Sakakibara, N.; Manecke, G.R.; Thistlethwaite, P.A.; Kerr, K.M.; Channick, R.N.; Fedullo, P.F.; Auger, W.R. Pulmonary endarterectomy: Experience and lessons learned in 1500 cases. *Ann. Thorac. Surg.* **2003**, *76*, 1457–1462; discussion 1462–1464. [[CrossRef](#)]
66. Madani, M.M.; Auger, W.R.; Pretorius, V.; Sakakibara, N.; Kerr, K.M.; Kim, N.H.; Fedullo, P.F.; Jamieson, S.W. Pulmonary endarterectomy: Recent changes in a single institution’s experience of more than 2700 patients. *Ann. Thorac. Surg.* **2012**, *94*, 97–103; discussion 103. [[CrossRef](#)]
67. Cannon, J.E.; Su, L.; Kiely, D.G.; Page, K.; Toshner, M.; Swietlik, E.; Treacy, C.; Ponnaberanam, A.; Condliffe, R.; Sheares, K.; et al. Dynamic Risk Stratification of Patient Long-Term Outcome After Pulmonary Endarterectomy: Results From the United Kingdom National Cohort. *Circulation* **2016**, *133*, 1761–1771. [[CrossRef](#)]
68. Brookes, J.D.L.; Li, C.; Chung, S.T.W.; Brookes, E.M.; Williams, M.L.; McNamara, N.; Martin-Suarez, S.; Loforte, A. Pulmonary thromboendarterectomy for chronic thromboembolic pulmonary hypertension: A systematic review. *Ann. Cardiothorac. Surg.* **2022**, *11*, 68–81. [[CrossRef](#)]
69. Martin-Suarez, S.; Gliozzi, G.; Cavalli, G.G.; Orioli, V.; Loforte, A.; Pastore, S.; Rossi, B.; Zardin, D.; Galiè, N.; Palazzini, M.; et al. Is Pulmonary Artery Pulsatility Index (PAPi) a Predictor of Outcome after Pulmonary Endarterectomy? *J. Clin. Med.* **2022**, *11*, 4353. [[CrossRef](#)]
70. Bonno, E.L.; Viray, M.C.; Jackson, G.R.; Houston, B.A.; Tedford, R.J. Modern Right Heart Catheterization: Beyond Simple Hemodynamics. *Adv. Pulm. Hypertens.* **2020**, *19*, 6–15. [[CrossRef](#)]
71. Richter, M.J.; Hsu, S.; Yogeswaran, A.; Husain-Syed, F.; Vadász, I.; Ghofrani, H.A.; Naeije, R.; Harth, S.; Grimminger, F.; Seeger, W.; et al. Right ventricular pressure-volume loop shape and systolic pressure change in pulmonary hypertension. *Am. J. Physiol. Lung Cell Mol. Physiol.* **2021**, *320*, L715–L725. [[CrossRef](#)] [[PubMed](#)]
72. Hunter, K.S.; Lee, P.-F.; Lanning, C.J.; Ivy, D.D.; Kirby, K.S.; Claussen, L.R.; Chan, K.C.; Shandas, R. Pulmonary vascular input impedance is a combined measure of pulmonary vascular resistance and stiffness and predicts clinical outcomes better than pulmonary vascular resistance alone in pediatric patients with pulmonary hypertension. *Am. Heart J.* **2008**, *155*, 166–174. [[CrossRef](#)] [[PubMed](#)]
73. Klok, F.A.; Ageno, W.; Ay, C.; Bäck, M.; Barco, S.; Bertolotti, L.; Becattini, C.; Carlsen, J.; Delcroix, M.; van Es, N.; et al. Optimal follow-up after acute pulmonary embolism: A position paper of the European Society of Cardiology Working Group on Pulmonary Circulation and Right Ventricular Function, in collaboration with the European Society of Cardiology Working Group on Atherosclerosis and Vascular Biology, endorsed by the European Respiratory Society. *Eur. Heart J.* **2022**, *43*, 183–189. [[PubMed](#)]
74. Parasuraman, S.; Walker, S.; Loudon, B.L.; Gollop, N.D.; Wilson, A.M.; Lowery, C.; Frenneaux, M.P. Assessment of pulmonary artery pressure by echocardiography—A comprehensive review. *Int. J. Cardiol. Heart Vasc.* **2016**, *12*, 45–51. [[CrossRef](#)] [[PubMed](#)]
75. Rudski, L.G.; Lai, W.W.; Afilalo, J.; Hua, L.; Handschumacher, M.D.; Chandrasekaran, K.; Solomon, S.D.; Louie, E.K.; Schiller, N.B. Guidelines for the echocardiographic assessment of the right heart in adults: A report from the American Society of Echocardiography endorsed by the European Association of Echocardiography, a registered branch of the European Society of Cardiology, and the Canadian Society of Echocardiography. *J. Am. Soc. Echocardiogr.* **2010**, *23*, 685–713; quiz 786–788.
76. Lang, R.M.; Badano, L.P.; Mor-Avi, V.; Afilalo, J.; Armstrong, A.; Ernande, L.; Flachskampf, F.A.; Foster, E.; Goldstein, S.A.; Kuznetsova, T.; et al. Recommendations for cardiac chamber quantification by echocardiography in adults: An update from the American Society of Echocardiography and the European Association of Cardiovascular Imaging. *J. Am. Soc. Echocardiogr.* **2015**, *28*, 1–39.e14. [[CrossRef](#)]

77. Tossavainen, E.; Söderberg, S.; Grönlund, C.; Gonzalez, M.; Henein, M.Y.; Lindqvist, P. Pulmonary artery acceleration time in identifying pulmonary hypertension patients with raised pulmonary vascular resistance. *Eur. Heart J. Cardiovasc. Imaging* **2013**, *14*, 890–897. [[CrossRef](#)]
78. Lee, J.H.; Park, J.H. Strain Analysis of the Right Ventricle Using Two-dimensional Echocardiography. *J. Cardiovasc. Imaging* **2018**, *26*, 111–124. [[CrossRef](#)]
79. Ruigrok, D.; Handoko, M.L.; Meijboom, L.J.; Nossent, E.J.; Boonstra, A.; Braams, N.J.; van Wezenbeek, J.; Tepaske, R.; Tuinman, P.R.; Heunks, L.M.; et al. Noninvasive follow-up strategy after pulmonary endarterectomy for chronic thromboembolic pulmonary hypertension. *ERJ Open Res.* **2022**, *8*, 00564–02021. [[CrossRef](#)]
80. Freed, B.H.; Collins, J.D.; François, C.J.; Barker, A.J.; Cuttica, M.J.; Chesler, N.C.; Markl, M.; Shah, S.J. MR and CT Imaging for the Evaluation of Pulmonary Hypertension. *JACC Cardiovasc. Imaging* **2016**, *9*, 715–732. [[CrossRef](#)]
81. Condliffe, R.; Kiely, D.G.; Gibbs, J.S.R.; Corris, P.A.; Peacock, A.J.; Jenkins, D.P.; Hodgkins, D.; Goldsmith, K.; Hughes, R.J.; Sheares, K.; et al. Improved outcomes in medically and surgically treated chronic thromboembolic pulmonary hypertension. *Am. J. Respir. Crit. Care Med.* **2008**, *177*, 1122–1127. [[CrossRef](#)] [[PubMed](#)]
82. Ishida, K.; Masuda, M.; Tanaka, H.; Imamaki, M.; Katsumata, M.; Maruyama, T.; Miyazaki, M. Mid-term results of surgery for chronic thromboembolic pulmonary hypertension. *Interact. Cardiovasc. Thorac. Surg.* **2009**, *9*, 626–629. [[CrossRef](#)] [[PubMed](#)]
83. Dittrich, H.C.; Nicod, P.H.; Chow, L.C.; Chappuis, F.P.; Moser, K.M.; Peterson, K.L. Early changes of right heart geometry after pulmonary thromboendarterectomy. *J. Am. Coll. Cardiol.* **1988**, *11*, 937–943. [[CrossRef](#)] [[PubMed](#)]
84. Dittrich, H.C.; Chow, L.C.; Nicod, P.H. Early improvement in left ventricular diastolic function after relief of chronic right ventricular pressure overload. *Circulation* **1989**, *80*, 823–830. [[CrossRef](#)] [[PubMed](#)]
85. D’Armini, A.M.; Zanotti, G.; Ghio, S.; Magrini, G.; Pozzi, M.; Scelsi, L.; Meloni, G.; Klersy, C.; Viganò, M. Reverse right ventricular remodeling after pulmonary endarterectomy. *J. Thorac. Cardiovasc. Surg.* **2007**, *133*, 162–168. [[CrossRef](#)] [[PubMed](#)]
86. Reesink, H.J.; Marcus, J.T.; Tulevski, I.I.; Jamieson, S.; Kloek, J.J.; Noordegraaf, A.V.; Bresser, P. Reverse right ventricular remodeling after pulmonary endarterectomy in patients with chronic thromboembolic pulmonary hypertension: Utility of magnetic resonance imaging to demonstrate restoration of the right ventricle. *J. Thorac. Cardiovasc. Surg.* **2007**, *133*, 58–64. [[CrossRef](#)]
87. Iino, M.; Dymarkowski, S.; Chaothawee, L.; Delcroix, M.; Bogaert, J. Time course of reversed cardiac remodeling after pulmonary endarterectomy in patients with chronic pulmonary thromboembolism. *Eur. Radiol.* **2008**, *18*, 792–799. [[CrossRef](#)]
88. Skoro-Sajer, N.; Marta, G.; Gerges, C.; Hlavin, G.; Nierlich, P.; Taghavi, S.; Sadushi-Kolici, R.; Klepetko, W.; Lang, I.M. Surgical specimens, haemodynamics and long-term outcomes after pulmonary endarterectomy. *Thorax* **2014**, *69*, 116–122. [[CrossRef](#)]
89. Hayashi, H.; Ning, Y.; Kurlansky, P.; Vaynrub, A.; Bacchetta, M.; Rosenzweig, E.B.; Takeda, K. Characteristics and prognostic significance of right heart remodeling and tricuspid regurgitation after pulmonary endarterectomy. *J. Thorac. Cardiovasc. Surg.* **2022**. [[CrossRef](#)]
90. Mauritz, G.-J.; Vonk-Noordegraaf, A.; Kind, T.; Surie, S.; Kloek, J.J.; Bresser, P.; Saouti, N.; Bosboom, J.; Westerhof, N.; Marcus, J.T. Pulmonary endarterectomy normalizes interventricular dyssynchrony and right ventricular systolic wall stress. *J. Cardiovasc. Magn. Reson.* **2012**, *14*, 5. [[CrossRef](#)]
91. Waziri, F.; Ringgaard, S.; Mellekjær, S.; Bøgh, N.; Kim, W.Y.; Clemmensen, T.S.; Hjortdal, V.E.; Nielsen, S.L.; Poulsen, S.H. Long-term changes of right ventricular myocardial deformation and remodeling studied by cardiac magnetic resonance imaging in patients with chronic thromboembolic pulmonary hypertension following pulmonary thromboendarterectomy. *Int. J. Cardiol.* **2020**, *300*, 282–288. [[CrossRef](#)] [[PubMed](#)]
92. Surie, S.; Bouma, B.; Bruin-Bon, R.A.; Hardziyenka, M.; Kloek, J.J.; Van der Plas, M.N.; Reesink, H.J.; Bresser, P. Time course of restoration of systolic and diastolic right ventricular function after pulmonary endarterectomy for chronic thromboembolic pulmonary hypertension. *Am. Heart J.* **2011**, *161*, 1046–1052. [[CrossRef](#)] [[PubMed](#)]
93. Fukui, S.; Ogo, T.; Morita, Y.; Tsuji, A.; Tateishi, E.; Ozaki, K.; Sanda, Y.; Fukuda, T.; Yasuda, S.; Ogawa, H.; et al. Right ventricular reverse remodelling after balloon pulmonary angioplasty. *Eur. Respir. J.* **2014**, *43*, 1394–1402. [[CrossRef](#)]
94. Broch, K.; Murbraech, K.; Ragnarsson, A.; Gude, E.; Andersen, R.; Fiane, A.E.; Andreassen, J.; Aakhus, S.; Andreassen, A.K. Echocardiographic evidence of right ventricular functional improvement after balloon pulmonary angioplasty in chronic thromboembolic pulmonary hypertension. *J. Heart Lung Transplant.* **2015**, *35*, 80–86. [[CrossRef](#)]
95. Tsugu, T.; Murata, M.; Kawakami, T.; Yasuda, R.; Tokuda, H.; Minakata, Y.; Tamura, Y.; Kataoka, M.; Hayashida, K.; Tsuruta, H.; et al. Significance of echocardiographic assessment for right ventricular function after balloon pulmonary angioplasty in patients with chronic thromboembolic induced pulmonary hypertension. *Am. J. Cardiol.* **2015**, *115*, 256–261. [[CrossRef](#)] [[PubMed](#)]
96. Sato, H.; Ota, H.; Sugimura, K.; Aoki, T.; Tatebe, S.; Miura, M.; Yamamoto, S.; Yaoita, N.; Suzuki, H.; Satoh, K.; et al. Balloon Pulmonary Angioplasty Improves Biventricular Functions and Pulmonary Flow in Chronic Thromboembolic Pulmonary Hypertension. *Circ. J.* **2016**, *80*, 1470–1477. [[CrossRef](#)]
97. Yamasaki, Y.; Nagao, M.; Abe, K.; Hosokawa, K.; Kawanami, S.; Kamitani, T.; Yamanouchi, T.; Horimoto, K.; Yabuuchi, H.; Honda, H. Balloon pulmonary angioplasty improves interventricular dyssynchrony in patients with inoperable chronic thromboembolic pulmonary hypertension: A cardiac MR imaging study. *Int. J. Cardiovasc. Imaging* **2016**, *33*, 229–239. [[CrossRef](#)]
98. Schoenfeld, C.; Hinrichs, J.B.; Olsson, K.M.; Kuettner, M.-A.; Renne, J.; Kaireit, T.; Czerner, C.; Wacker, F.; Hoepfer, M.M.; Meyer, B.C.; et al. Cardio-pulmonary MRI for detection of treatment response after a single BPA treatment session in CTEPH patients. *Eur. Radiol.* **2018**, *29*, 1693–1702. [[CrossRef](#)]

99. Marra, A.M.; Egenlauf, B.; Ehlken, N.; Fischer, C.; Eichstaedt, C.; Nagel, C.; Bossone, E.; Cittadini, A.; Halank, M.; Gall, H.; et al. Change of right heart size and function by long-term therapy with riociguat in patients with pulmonary arterial hypertension and chronic thromboembolic pulmonary hypertension. *Int. J. Cardiol.* **2015**, *195*, 19–26. [[CrossRef](#)]
100. Murata, M.; Kawakami, T.; Kataoka, M.; Kohno, T.; Itabashi, Y.; Fukuda, K. Riociguat, a soluble guanylate cyclase stimulator, ameliorates right ventricular contraction in pulmonary arterial hypertension. *Pulm. Circ.* **2017**, *8*, 2045893217746111. [[CrossRef](#)]
101. Murata, M.; Kawakami, T.; Kataoka, M.; Moriyama, H.; Hiraide, T.; Kimura, M.; Endo, J.; Kohno, T.; Itabashi, Y.; Fukuda, K. Clinical Significance of Guanylate Cyclase Stimulator, Riociguat, on Right Ventricular Functional Improvement in Patients with Pulmonary Hypertension. *Cardiology* **2020**, *146*, 130–136. [[CrossRef](#)] [[PubMed](#)]
102. Rézaiguia-Delclaux, S.; Haddad, F.; Pilorge, C.; Amsallem, M.; Fadel, E.; Stéphan, F. Limitations of right ventricular annular parameters in the early postoperative period following pulmonary endarterectomy: An observational study. *Interact. Cardiovasc. Thorac. Surg.* **2020**, *31*, 191–198. [[CrossRef](#)] [[PubMed](#)]
103. Corsico, A.G.; D'Armini, A.M.; Conio, V.; Sciortino, A.; Pin, M.; Grazioli, V.; Di Vincenzo, G.; Di Domenica, R.; Celentano, A.; Vanini, B.; et al. Persistent exercise limitation after successful pulmonary endarterectomy: Frequency and determinants. *Respir. Res.* **2019**, *20*, 34. [[CrossRef](#)] [[PubMed](#)]
104. Claessen, G.; La Gerche, A.; Dymarkowski, S.; Claus, P.; Delcroix, M.; Heidbuchel, H. Pulmonary vascular and right ventricular reserve in patients with normalized resting hemodynamics after pulmonary endarterectomy. *J. Am. Heart Assoc.* **2015**, *4*, e001602. [[CrossRef](#)] [[PubMed](#)]
105. Godinas, L.; Verbelen, T.; Delcroix, M. Residual pulmonary hypertension after pulmonary thromboendarterectomy: Incidence, pathogenesis and therapeutic options. *Ann. Cardiothorac. Surg.* **2022**, *11*, 163–165. [[CrossRef](#)]
106. Ghio, S.; Morsolini, M.; Corsico, A.; Klersy, C.; Mattiucci, G.; Raineri, C.; Scelsi, L.; Vistarini, N.; Visconti, L.O.; D'Armini, A.M. Pulmonary arterial compliance and exercise capacity after pulmonary endarterectomy. *Eur. Respir. J.* **2014**, *43*, 1403–1409. [[CrossRef](#)]
107. Hardziyenka, M.; Reesink, H.J.; Bouma, B.J.; de Bruin-Bon, H.R.; Campian, M.E.; Tanck, M.W.; Brink, R.B.V.D.; Kloek, J.J.; Tan, H.L.; Bresser, P. A novel echocardiographic predictor of in-hospital mortality and mid-term haemodynamic improvement after pulmonary endarterectomy for chronic thrombo-embolic pulmonary hypertension. *Eur. Heart J.* **2007**, *28*, 842–849. [[CrossRef](#)]
108. Surie, S.; van der Plas, M.N.; Marcus, J.T.; Kind, T.; Kloek, J.J.; Vonk-Noordegraaf, A.; Bresser, P. Effect of pulmonary endarterectomy for chronic thromboembolic pulmonary hypertension on stroke volume response to exercise. *Am. J. Cardiol.* **2014**, *114*, 136–140. [[CrossRef](#)]
109. Maschke, S.K.; Schoenfeld, C.O.; Kaireit, T.F.; Cebotari, S.; Olsson, K.; Hoepfer, M.; Wacker, F.; Vogel-Claussen, J. MRI-derived Regional Biventricular Function in Patients with Chronic Thromboembolic Pulmonary Hypertension Before and After Pulmonary Endarterectomy. *Acad. Radiol.* **2018**, *25*, 1540–1547. [[CrossRef](#)]
110. Brenot, P.; Jaïs, X.; Taniguchi, Y.; Alonso, C.G.; Gerardin, B.; Mussot, S.; Mercier, O.; Fabre, D.; Parent, F.; Jevnikar, M.; et al. French experience of balloon pulmonary angioplasty for chronic thromboembolic pulmonary hypertension. *Eur. Respir. J.* **2019**, *53*, 1802095. [[CrossRef](#)]
111. Mizoguchi, H.; Ogawa, A.; Munemasa, M.; Mikouchi, H.; Ito, H.; Matsubara, H. Refined balloon pulmonary angioplasty for inoperable patients with chronic thromboembolic pulmonary hypertension. *Circ. Cardiovasc. Interv.* **2012**, *5*, 748–755. [[CrossRef](#)] [[PubMed](#)]
112. DaRocha, S.; Pietura, R.; Banaszkiwicz, M.; Pietrasik, A.; Kownacki, Ł.; Torbicki, A.; Kurzyna, M. Balloon Pulmonary Angioplasty with Stent Implantation as a Treatment of Proximal Chronic Thromboembolic Pulmonary Hypertension. *Diagnostics* **2020**, *10*, 363. [[CrossRef](#)] [[PubMed](#)]
113. Godinas, L.; Bonne, L.; Budts, W.; Belge, C.; Leys, M.; Delcroix, M.; Maleux, G. Balloon Pulmonary Angioplasty for the Treatment of Nonoperable Chronic Thromboembolic Pulmonary Hypertension: Single-Center Experience with Low Initial Complication Rate. *J. Vasc. Interv. Radiol.* **2019**, *30*, 1265–1272. [[CrossRef](#)] [[PubMed](#)]
114. Sumimoto, K.; Tanaka, H.; Mukai, J.; Yamashita, K.; Tanaka, Y.; Shono, A.; Suzuki, M.; Yokota, S.; Suto, M.; Takada, H.; et al. Effects of balloon pulmonary angioplasty for chronic thromboembolic pulmonary hypertension on remodeling in right-sided heart. *Int. J. Cardiovasc. Imaging* **2020**, *36*, 1053–1060. [[CrossRef](#)] [[PubMed](#)]
115. Kanar, B.G.; Mutlu, B.; Atas, H.; Akaslan, D.; Yildizeli, B. Improvements of right ventricular function and hemodynamics after balloon pulmonary angioplasty in patients with chronic thromboembolic pulmonary hypertension. *Echocardiography* **2019**, *36*, 2050–2056. [[CrossRef](#)]
116. Li, W.; Yang, T.; Quan, R.L.; Chen, X.X.; An, J.; Zhao, Z.H.; Liu, Z.H.; Xiong, C.M.; He, J.G.; Gu, Q. Balloon pulmonary angioplasty reverse right ventricular remodelling and dysfunction in patients with inoperable chronic thromboembolic pulmonary hypertension: A systematic review and meta-analysis. *Eur. Radiol.* **2021**, *31*, 3898–3908. [[CrossRef](#)]
117. Schermuly, R.T.; Stasch, J.-P.; Pullamsetti, S.S.; Middendorff, R.; Muller, D.; Schluter, K.-D.; Dingendorf, A.; Hackemack, S.; Kolosionek, E.; Kaulen, C.; et al. Expression and function of soluble guanylate cyclase in pulmonary arterial hypertension. *Eur. Respir. J.* **2008**, *32*, 881–891. [[CrossRef](#)]
118. Weissmann, N.; Lobo, B.; Pichl, A.; Parajuli, N.; Seimetz, M.; Puig-Pey, R.; Ferrer, E.; Peinado, V.I.; Domínguez-Fandos, D.; Fysikopoulos, A.; et al. Stimulation of soluble guanylate cyclase prevents cigarette smoke-induced pulmonary hypertension and emphysema. *Am. J. Respir. Crit. Care Med.* **2014**, *189*, 1359–1373. [[CrossRef](#)]

119. Pradhan, K.; Sydykov, A.; Tian, X.; Mamazhakypov, A.; Neupane, B.; Luitel, H.; Weissmann, N.; Seeger, W.; Grimminger, F.; Kretschmer, A.; et al. Soluble guanylate cyclase stimulator riociguat and phosphodiesterase 5 inhibitor sildenafil ameliorate pulmonary hypertension due to left heart disease in mice. *Int. J. Cardiol.* **2016**, *216*, 85–91. [[CrossRef](#)]
120. Rai, N.; Veeroju, S.; Schymura, Y.; Janssen, W.; Wietelmann, A.; Kojonazarov, B.; Weissmann, N.; Stasch, J.P.; Ghofrani, H.A.; Seeger, W.; et al. Effect of Riociguat and Sildenafil on Right Heart Remodeling and Function in Pressure Overload Induced Model of Pulmonary Arterial Banding. *Biomed Res. Int.* **2018**, *2018*, 3293584.
121. Kim, N.H.; D'Armini, A.M.; Grimminger, F.; Grünig, E.; Hoeper, M.M.; Jansa, P.; Mayer, E.; Neurohr, C.; Simonneau, G.; Torbicki, A.; et al. Haemodynamic effects of riociguat in inoperable/recurrent chronic thromboembolic pulmonary hypertension. *Heart* **2016**, *103*, 599–606. [[CrossRef](#)] [[PubMed](#)]
122. Simonneau, G.; D'Armini, A.M.; Ghofrani, A.; Grimminger, F.; Jansa, P.; Kim, N.H.; Mayer, E.; Pulido, T.; Wang, C.; Colorado, P.; et al. Predictors of long-term outcomes in patients treated with riociguat for chronic thromboembolic pulmonary hypertension: Data from the CHEST-2 open-label, randomised, long-term extension trial. *Lancet Respir. Med.* **2016**, *4*, 372–380. [[CrossRef](#)] [[PubMed](#)]
123. Marra, A.M.; Halank, M.; Benjamin, N.; Bossone, E.; Cittadini, A.; Eichstaedt, C.A.; Egenlauf, B.; Harutyunova, S.; Fischer, C.; Gall, H.; et al. Right ventricular size and function under riociguat in pulmonary arterial hypertension and chronic thromboembolic pulmonary hypertension (the RIVER study). *Respir. Res.* **2018**, *19*, 258. [[CrossRef](#)] [[PubMed](#)]
124. Aoki, T.; Sugimura, K.; Terui, Y.; Tatebe, S.; Fukui, S.; Miura, M.; Yamamoto, S.; Yaoita, N.; Suzuki, H.; Sato, H.; et al. Beneficial effects of riociguat on hemodynamic responses to exercise in CTEPH patients after balloon pulmonary angioplasty—A randomized controlled study. *IJC Heart Vasc.* **2020**, *29*, 100579. [[CrossRef](#)] [[PubMed](#)]
125. Darocha, S.; Banaszkiwicz, M.; Pietrasik, A.; Piłka, M.; Florczyk, M.; Wieteska, M.; Dobosiewicz, A.; Szmit, S.; Torbicki, A.; Kurzyna, M. Sequential treatment with sildenafil and riociguat in patients with persistent or inoperable chronic thromboembolic pulmonary hypertension improves functional class and pulmonary hemodynamics. *Int. J. Cardiol.* **2018**, *269*, 283–288. [[CrossRef](#)] [[PubMed](#)]
126. Jaïs, X.; Brenot, P.; Bouvaist, H.; Jevnikar, M.; Canuet, M.; Chabanne, C.; Chaouat, A.; Cottin, V.; De Groote, P.; Favrolt, N.; et al. Balloon pulmonary angioplasty versus riociguat for the treatment of inoperable chronic thromboembolic pulmonary hypertension (RACE): A multicentre, phase 3, open-label, randomised controlled trial and ancillary follow-up study. *Lancet Respir. Med.* **2022**, *10*, 961–971. [[CrossRef](#)]

Disclaimer/Publisher's Note: The statements, opinions and data contained in all publications are solely those of the individual author(s) and contributor(s) and not of MDPI and/or the editor(s). MDPI and/or the editor(s) disclaim responsibility for any injury to people or property resulting from any ideas, methods, instructions or products referred to in the content.